Migration of organic contaminants through paper and plastic packaging

By

Ineke Tiggelman

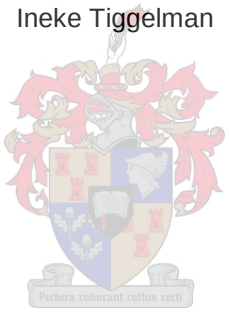

Thesis presented in partial fulfillment of the requirements for the degree of

Master of Science (Polymer Science)

at

University of Stellenbosch

Promotor: Prof. H. Pasch

Co-promotor: Dr. P. C. Hartmann

March 2012

Declaration

I, the undersigned, hereby declare that the work contained in this dissertation is my own original work and that I have not previously in its entirety or in part submitted it at any university for a degree.

Signature: **Date: March 2012**

Ineke Tiggelman

Abstract

The presence of mineral oils in dry foodstuff was found to originate from the packaging materials, namely, paperboard manufactured from recovered fibres, and these oils subsequently migrate to the foodstuff via the vapour phase. The presence of mineral oils in food is of concern as it originates from the use of paper products not originally intended for food contact applications, i.e., before the paper is subjected to a suitable recycling process. These mineral oils consist of technical grade compounds which may contain aromatic compounds and other components with unknown toxicological effects. Although the related authorities are currently considering the safe and legal limits of these contaminants in foodstuffs, as well as establishing a standardised test method for monitoring mineral oils in food and packaging materials, paperboard manufacturers wish to ensure that their products are safe for food contact applications. Since recycling is unavoidable, particularly from an ecological and economical point of view, one of the proposed solutions the industry is focussing on is the use of a functional barrier towards mineral oils – be it an inner bag as a direct food-contact surface, or a barrier coating directly applied on the inner side of the paperboard.

In this study, a permeation test method was established, and developed, to evaluate the transmission rate of a volatile organic compound, acting as a mineral oil simulant, through model paper and plastic packaging materials. This was correlated to the transmission rate of actual mineral oil through the packaging materials, and therefore used as a highly accelerated tool to characterise packaging materials in relation to their barrier properties. The test method, referred to as the “heptane vapour transmission rate,” was subsequently used to derive the required transport parameters’ characteristics of each of the tested materials, which enabled an evaluation of the potential shelf-life of the packaged product. This research demonstrated that barrier-coated paperboards have the ability to behave in the same way as, and often even better than, commercial plastic films, towards the migration of mineral oil.

Detailed information on the interaction between the packaging materials and mineral oil simulant, *n*-heptane, was acquired from gravimetric sorption. Insight was obtained into a material’s ability to function as a mineral oil barrier. It was established that the quick and easy permeation method was sufficient for evaluating packaging materials as potential mineral oil barriers, and resulted in the determination of transport parameters that were higher than that obtained by sorption. The obtained transport parameters could therefore be considered a worst case scenario when predicting the package content shelf-life.

Opsomming

Daar is voorheen bevind dat die teenwoordigheid van mineraalolies in droë voedsel afkomstig is van die verpakkingsmateriaal, naamlik karton, wat vervaardig is van herwonne papierprodukte, en daarna migreer die olies na die voedsel deur die gasfase. Die teenwoordigheid van hierdie mineraalolies in kos wek groot kommer aangesien dit afkomstig is van papierprodukte wat nie oorspronklik bedoel is vir voedselkontak voor die herwinningsproses nie. Die olies bestaan uit industriële graad mineraalolies wat moontlik aromatiese verbindings asook ander komponente bevat waarvan die toksiekologiese effekte onbekend is. Terwyl die betrokke owerhede tans besig is om die veilige en wettige grense van hierdie kontaminante in voedsel te oorweeg, asook die vestigting van 'n gestandaardiseerde toetsmetode vir die kontrole van mineraalolies in die voedsel-verpakkingsmateriaal-kombinasie, wil karton- en papiervervaardigers graag verseker dat hul produkte veilig is vir voedselkontak. Siende dat herwinning onvermydelik is vanuit 'n ekologiese en ekonomiese oogpunt, is een van die voorgestelde oplossings in die bedryf om te fokus op die gebruik van 'n funksionele keerfilm ten opsigte van mineraalolies, wat ‘n sakkie binne-in die karton, wat dien as die direkte kos-kontakoppervlak, of 'n keerlaag, wat direk aangewend word op die binnekant van die karton, kan behels.

Hierdie studie ondersoek die daarstel en deursypelingsontwikkeling van 'n toetsmetode om die oordragtempo van 'n vlugtige organiese verbinding, wat optree as 'n mineraalolie simulant, deur middel van model papier- en plastiekverpakkingsmateriale, te evalueer. Dit stem ooreen met die oordragtempo van werklike mineraalolies deur die verpakkingsmateriaal en kan dus gebruik word as 'n hoogs versnelde instrument om verpakkingsmateriale te karakteriseer met betrekking tot hul keereienskappe. Die toetsmetode, die sogenaamde "heptaangasoordragtempo," is vervolgens gebruik om die vereiste oordragparameters af te lei wat kenmerkend is van elk van die geëvalueerde verpakkingsmateriale en wat sodoende gebruik kon word om die potensiële raklewe van die verpakte produk te bepaal. Hierdie navorsing het getoon dat kartonprodukte met ‘n keerlaag die vermoë het om dieselfde op te tree as kommersiële plastiekfilms en dikwels selfs beter, ten opsigte van die migrasie van mineraalolies.

Gedetailleerde inligting oor die interaksie tussen die verpakkingsmateriale en mineraalolie simulant, *n*-heptaan, is verkry vanaf gravimetriese sorpsie. Dit gee insig in 'n materiaal se vermoë om te funksioneer as 'n mineraalolie-keermiddel. Daar is vasgestel dat die vinnige en maklike deurwerking metode voldoende is vir die evaluering van verpakkingsmateriale as potensiële mineraalolie-keermiddels, en verleen oordragparameters wat hoër is as dié verkry deur sorpsie. Hierdie oordragparameters kan dus as 'n ergste scenario vir die voorspelling van die raklewe van ‘n verpakte produk beskou word.

Acknowledgements

My promotors, Prof. H. Pasch and Dr P. Hartmann, for guidance and academic support

Dr V. Cloete, for giving me the opportunity to further my studies

Mpact Limited, for financially supporting the research

Mpact R & D group, for continuous assistance

Dr M. Hurndall, for editorial assistance

Eddson Zengeni, for advice

Corné Yzelle, for assistance with mathematical work

Henk Tiggelman, for unlimited support

Family and friends, for encouragement

Table of Contents

List of Figures

List of Schemes

List of Tables

List of Symbols

P	Permeability coefficient
D	Diffusion coefficient
S	Solubility coefficient
p	Pressure
c	Concentration
$K_{P/F}$	Partition coefficient
V_F	Volume of food
V_P	Volume of polymer
ρ	Density
A	Area

List of Abbreviations

BfR	German Federal Institute for Risk Assessment
DMS	Dual mode sorption
HDPE	High density polyethylene
HPLC	High performance liquid chromatography
HVTR	Heptane vapour transmission rate
LDPE	Low density polyethylene
mbar	Millibar
MO	Mineral oil
MOAH	Mineral oil aromatic hydrocarbons
MOSH	Mineral oil saturated hydrocarbons
MOVTR	Mineral oil vapour transmission rate
OML	Overall migration limit
PB	Paperboard
PE	polyethylene
PET	Polyethylene terephthalate
PP	Polypropylene
SML	Specific migration limit
STP	Standard temperature and pressure
VOC	Volatile organic compound

Chapter 1

Introduction and objectives

1.1 Introduction

Recent publications focused the attention of the paper, packaging and ink industries on the presence of mineral oils in food packaging and their migration into food in alarmingly high concentrations. No official method has yet been recognised by standardization authorities for measuring the mineral oil content in either packaging materials or foods, but at present the method of choice is that published by Dr K. Grob of the Official Food Control Authority of the Canton of Zurich (Switzerland) [1, 2]. This method measures the absolute concentration of mineral oils in either food packaging or contaminated food. It involves the extraction of hydrocarbons with a solvent, followed by analysis via on-line high performance liquid chromatography-gas chromatography (HPLC-GC). This is a quite complex method that requires expensive equipment and highly knowledgeable operators. There is, therefore, the need for a simple test to predetermine whether paper and board manufacturers' products are safe, or comply with safety regulations, and which is easy to carry out on-site for quality control purposes.

Before the publication of these findings, mineral oils in food and food contact materials were not a major problem, as some well-known mineral hydrocarbons are food grade approved and commonly used in food contact applications. For this reason, no suitable quality control test methods exist to manage the migration of mineral oils from packaging products into foodstuffs. This study aims at developing an analytical test method for the evaluation of barrier properties of packaging material towards mineral oil. The method involves using accelerated conditions, based on the permeation method for measuring the transmission rate of the organic compounds through barrier materials. The new test method should provide a quick and easy means to test the performance of paperboard in terms of its potential to prevent the migration of mineral oil from primary, secondary or tertiary packaging into foodstuff via the vapour phase. The method should be used for evaluating the efficiency of functional barrier coatings in protecting foodstuff from mineral oil contamination, and also assist in the product development of coating formulations. Furthermore, it should enable papermakers to use this test method as a means of quality control for mineral oil barrier properties.

1.2 Objectives

This study aims mainly at developing a robust analytical method that allows simulating the migration of organic contaminants through model food packaging substrates. This was achieved through the following objectives:

1.2.1 To set up a simple permeation method that simulates the transmission of organic vapour under conditions characteristic of dry food packaging.

1.2.2 To evaluate the barrier properties of model polymeric materials towards organic vapour using the newly developed method of analysis, through:

a. model polymeric films
b. barrier-coated paperboard.

1.2.3 To analyse organic vapour sorption of model polymeric materials for correlation with results from the new test method, to better understand mineral oil migration through barrier-coated paperboard.

1.3 Layout of thesis

Chapter 1 of this thesis contains a short introduction to the commencement of the study, as well as the objectives. The theoretical aspects facing this research are discussed in Chapter 2, focusing on food contamination through packaging materials and specific methods of analysis. Chapter 3 explains all experimental procedures followed for setting up and validating a new analytical test method. The transport parameters obtained with the new permeation test method are given and discussed in Chapter 4, and Chapter 5 involves validation of the new test method in relation to sorption results. Final conclusions and recommendations are given in Chapter 6.

References

1. Biedermann, M. and Grob, K., Is recycled newspaper suitable for food contact materials? Technical grade mineral oils from printing inks. *Eur. Food Res. Technol.,* (2010) 230: 785–796.

2. Vollmer, A., Biedermann, M., Grundbock, F., Ingenhoff, J.-E., Biedermann-Brem, S., Altkofer, W., and Grob, K., Migration of mineral oil from printed paperboard into dry foods: survey of the German market. *Eur. Food Res. Technol.,* (2011) 232: 175–182.

Chapter 2

Theoretical background

2.1 Introduction

The food packaging industry has long been aware of possible contamination of foods by compounds present in the packaging. For this reason all food packaging are subject to the regulations of food health and safety laws. No undesirable compounds may migrate from the packaging into the food and as a result cause any harm to the health of consumers, or even reduce the quality of the food. Recycling is encouraged extensively since it constitutes an economic way of ensuring the sustainability of our natural resources, and also to limit levels of solid waste going into landfill. Food packaging is often made of recycled materials as this has a significant economic benefit regarding food costs. However, the recycling process also introduces a number of undesirable, and often unknown, compounds into the final packaging that may potentially migrate into the food. Plastic packaging made from recycled waste can be regulated to some extent, but this can be more difficult in the case of recovered paper and board.

Recently, non-food grade hydrocarbons from mineral origin were found in paper packaging for food [1]. It has also been found that these compounds are able to migrate into the food itself [2]. A comprehensive study of the composition of these compounds present in paper packaging, and consequently in the packed food, has not been carried out due to the very complex mixtures involved, and also due to frequent changes in the content of recovered pulp. But its mere presence is still alarming, since previous studies on animals have shown that organ damage could occur with the accumulation of significant quantities of these materials in the body [3]. The German Federal Institute for Risk Assessment (BfR), who acts as a focal point between the European Food Safety Authority and the European Union federal ministries, was the first official organisation to announce the recent findings. They declared that more research needs to be done on the composition of mineral oils present in recycled paper and board, as well as on the toxicological effects on human health. In the mean time, while the food and packaging industry are expectantly waiting for proper legislation, the BfR has emphasised the importance of reducing the migration of mineral oils into food.

2.2 Common contaminants in paper and board

Paper and board products used in direct food contact applications are well-known. These include baking papers, filters, sugar bags, teabags, butter wrapping, baked goods, cartons for dry (cereals like oats) and frozen foods, paper plates and cups. A large portion of paper and board packaging intended for food is utilised with a coating or laminate barrier layer, usually for liquid packaging like milk and beverages. In such cases the food is not in direct contact with the paper, but rather in contact with a plastic or aluminium foil inner layer.

An evaluation of food packaging samples containing only virgin fibre showed that the concentration of chemicals with the ability to migrate into food was insignificant compared to that of samples with recycled fibre content [4]. Some of the earliest studies on recycled paperboard showed the presence of phthalates [5] and naphthalenes [6]. Phthalates, benzophenone, and diisopropyl naphthalenes (DIPNs) are considered the most profound contaminants in a wide range of paper samples tested [7]. Bisphenol A has also been found in recycled papers [4, 8]. The presence of potentially toxic compounds in paperboard, therefore, needs to be monitored for their amounts in the paper, but also in terms of their migration into foodstuff.

In Europe, the migration of contaminants from packaging materials into food is regulated by an overall migration limit (OML), which refers to the total migrating material, and the specific migration limit (SML), which refers to individual authorised compounds that are able to migrate into food. The OML currently has a limit of 60 mg/kg of food [4, 9]. The BfR set up requirements on food contact materials, including those for paper and board. These requirements include specifications on the types of raw materials, production aids, and specialty additives that are allowed to be used in paper or board that comes into direct contact with food. The contaminants causing concerns for health issues are listed in Table 2.1, and include heavy metals, colourants, primary aromatic amines (PAAs), polyaromatic hydrocarbons (PAHs), phthalates, benzophenone and a number of its derivatives, and bisphenol A, among others. Some of these contaminants are found only in paper and board packages produced from recovered fibre and, therefore, have a high probability of migrating into the foodstuff. These contaminants would not necessarily be present in packaging produced from virgin fibres. Some other contaminants mentioned in Table 2.1 are found mostly in foods where the paper or board packaging

comes into direct contact with moist or fatty foods and, therefore, most likely materialise in the food it contains.

Table 2.1: Restriction limits of contaminants in paper and board for food contact [10, 11]

Compounds	Limit in food (SML) [mg/kg food]	Limit in paper & board	♣/♦	Sources of contamination
Cadmium	-	0.5 mg/kg	♣	inks
Lead	-	3.0 mg/kg	♣	inks
Mercury	-	0.3 mg/kg	♣	inks
Pentachlorophenol	-	0.15 mg/kg		biocide [12]
Azo colourants (sum of listed aromatic amines)	-	0.1 mg/kg	♦ ♣	
Primary aromatic amines (PAAs)	< 0.01		♣	overprint varnishes; polyurethane adhesives
Dyes and colourants	-	No bleeding	♣	
Fluorescent whitening agents (FWAs)	-	No bleeding	♣	
Formaldehyde		1 mg/dm^2		dry strength resins and crosslinkers
Polycyclic aromatic hydrocarbons (sum of listed PAHs)	0.01	0.0016 mg/dm^2	♦	
Dibutylphthalate (DBP)	0.3	0.05 mg/dm^2	♦	plasticiser, additive in adhesives or printing inks [13]
Diisobutylphthalate (DiBP)	1.0	0.17 mg/dm^2	♦	plasticiser, a component in adhesives [5]
Sum of DBP + DiBP	1.0	0.17 mg/dm^2	♦	
Di(2-ethylhexyl)phthalate (DEHP)	1.5	0.25 mg/dm^2	♦	plasticiser in adhesives, component in defoamers [5]
Benzylbutylphthalate (BBP)	30	5 mg/dm^2	♦	
Diisononylphthalate (DiNP)	9.0	1.5 mg/dm^2	♦	Hot-melt adhesives
Diisodecylphthalate (DiDP)	9.0	1.5 mg/dm^2	♦	
4,4-bis(diethylamino) benzophenone (DEAB)	0.01	0.0016 mg/dm^2	♦ ♣	UV-cure ink photoinitiators [14]
4,4-bis(dimethylamino) benzophenone (DMAB or Michler's ketone)	0.01	0.0016 mg/dm^2	♦ ♣	UV-cure ink photoinitiators [14]

Benzophenone (BP)	0.6	0.1 mg/dm^2	♦	UV-cure ink photoinitiators, wetting agent for pigments, reactive solvent in inks [14, 15]
Sum: BP + hydroxy-benzophenone + 4-methylbenzophenone	0.6	0.1 mg/dm^2		
Diisopropylnaphthalene (DiPN)	-	As low as possible	♦	solvent in manufacture of carbonless and thermal copy paper [6]
Bisphenol A	0.6	0.1 mg/dm^2	♦ ♣	epoxy-phenolic resins used as binders in printing inks [8]

♣ Testing required only if paper/board is in direct contact with moist or fatty foodstuff.

♦ Found only in recovered paper and board, testing not required for 100% virgin products.

2.2.1 Sources of contamination

Table 2.1 lists the most common sources causing the presence of contaminants in paper and board packaging. One of the main culprits is printing inks, or rather components in printing inks. The printed surface of the food packaging is usually not in direct contact with the food itself, but migration of harmful components into the food may take place in the absence of a suitable barrier between the food and the printed surface. These inks may also find their way back into the food chain via recycling and subsequent production of food packages from recycled fibre. Other common sources of contamination are additives in adhesives utilised during the various converting processes, as well as additives utilised during the papermaking process itself.

2.2.2 Analytical identification of food contaminants

Migration/mass transfer of pollutants from plastic packaging into food has been studied extensively [16, 17]. However, since the matrices, types of contaminants, and types of packed foods in recycled paper and board differs from that of recycled plastics, there is no direct correlation established between migration through fibrous matrices and results obtained for plastic materials. Studies lead by Boccacci-Mariani were carried out with direct contact between the paperboard and dry foodstuffs, but also where there was no contact, i.e. an air-space existed between the paperboard and the food. They verified that diisopropyl naphthalenes in paper packaging transferred to the food via both mechanisms. Contamination of the food thus occurred by transfer from direct contact between the two components, but also through diffusion of DiPN throughout the gas phase, and subsequent migration into the food.

In addition, they have shown that foods with higher specific surface areas are more susceptible to migration [6].

Analytical test methods for naphthalenes include gas chromatography with flame ionization detection (GC-FID) [6], or high performance liquid chromatography (HPLC) with fluorescence detection [7]. Quantification of Bisphenol A in packaging products, or in foodstuff, are also carried out using HPLC with fluorescence detection [17]. Phthalates in paper, food, and food simulants have been extracted by a suitable solvent such as hexane, ethanol, ethylacetate, or acetonitrile, and identified by gas chromatography-mass spectrometry (GC/MS) using selective ion monitoring (SIM) detection [5, 7]. Benzophenone has been extracted from food and paper packaging and quantified using GC-FID [12] or GC/MS [14, 15]. Benzophenone has also been found to migrate from paper packaging into foodstuff, even at temperatures as low as –20℃. Po lyethylene (PE) inner liner does not prevent the migration of benzophenone, dimethylphthalate, or pentachlorophenol, although no significant migration of non-polar anthracene and methyl stearate has been observed through PE [12, 14]. Polypropylene (PP) has also proven not to be an effective barrier to migration of contaminants expected to be in recycled paper either [18]. Rapid test methods for identification and quantification of a combination of model compounds expected to be found in recycled paper, and thus also in the packaged food, have been developed using solvent extraction, followed by gas chromatography-electron capture detection (GC-ECD) [18], GC/MS [19], and GC-FID [13, 20, 21].

Quantification of the most common heavy metals of concern in food packaging applications mentioned in Table 2.1, is achieved by inductively coupled plasma-mass spectrometry (ICP-MS) for lead (Pb), cadmium (Cd) and mercury (Hg), or inductively coupled plasma-atomic emission spectroscopy (ICP-AES) for Pb and Cd [22]. ICP-MS is a very sensitive technique with very low detection limits, whereas ICP-AES is a more robust technique suitable for routine analyses. Other suitable methods include electrothermal atomic-absorption spectrophotometry (ETAAS) for Pb and Cd, and cold vapour-absorption spectrophotometry (CVAAS) for the determination of Hg, or x-ray fluorescence (XRF) analysis [23].

It has also been found that volatile contaminants in secondary packaging often used as transport packaging, such as corrugated boxes, are able to migrate through the primary packaging into food via the gas phase [19]. Transfer of more volatile substances occurs more rapidly than less volatile

substances. However, besides volatility, other factors, such as total storage time, temperature and concentration of the contaminants present in the packaging, also play a role in possible migration. This indicates that a compound with low volatility, but high in concentration, may start migrating to the food after longer periods of storage times. Paper with an ethylene-vinyl acetate coating as primary packaging did not act as a barrier for migration of contaminants such as benzophenone (intrinsic contaminant), and 2,4,6-trichloroanisole, or DIPN (surrogate contaminants) from secondary packaging [19]. PP film wrapping between primary and secondary packaging did not act as a proper barrier either, but did however reduce the rate of migration.

2.3 New contaminant identified: mineral oil

Recycling in the paper industry is encouraged as an economic way of ensuring the sustainability of our natural resources and also as a way of reducing the increasing levels of municipal solid waste. Food packaging is typically made of recycled materials as this has a favorable environmental impact and economical benefits such as the final cost of packaged articles. However, the recycling process may also introduce a number of undesirable, and often unknown, compounds into the final packaging.

Recently it was found that mineral oils originating from the recycled fibre in paperboard are able to migrate into food (packaged in recycled packaging) via the vapour phase [1]. This raised major concern, as these mineral hydrocarbons are often not food grade approved, and toxicological assessments of this complex mixture of compounds are still uncertain at present. For this reason, legislation has not been finalised regarding restriction limits in packaging products, but it was recommended that 0.01 mg per kg of bodyweight is a safe upper intake limit per day [2]. This corresponds to 0.6 mg/kg food, if it is assumed that an average person weighs 60kg and eats 1kg of contaminated food per day.

2.3.1 Definition of mineral oils

2.3.1.1 Mineral hydrocarbons

Mineral hydrocarbons are from petroleum origins, and thus consist of a complex mixture of hydrocarbons. Mineral hydrocarbons refer to [24, 25]:

- paraffin waxes or macrocrystalline waxes (these waxes have between 18-45 carbon atoms; they consists mainly of normal paraffins which are the straight chain alkanes, and isoparaffins

which are branched chains, and also cycloparaffins consisting of saturated cycloalkanes/rings with side chains, also known as naphthenic oils)

- intermediate waxes (these are similar to paraffin waxes in structure, but consist of a higher portion of the isoparaffins and cycloparaffins, and have a higher molecular mass with a number of carbon atoms of up to 60)
- microcrystalline waxes (also consist of normal paraffins but with more branched chains and higher molecular weights, carbon atoms between 30-85 or even more)
- mineral oils (these are classified by their viscosities and consist of low and medium viscosity oils with carbon atoms between 10-25, and high viscosity oils with about 30 carbon atoms)
- petrolatum (also known as petroleum jelly, consisting of a mixture of paraffin waxes, microcrystalline waxes, and mineral oils)

The boundaries between the abovementioned classes are not distinct, and due to the complex mixtures of an enormous amount of components involved, mineral hydrocarbons have not been well characterised and identified. Food grade mineral hydrocarbons are obtained from refining processes that remove all unsaturated and aromatic hydrocarbons. These materials can include petrolatum, paraffin and microcrystalline waxes, as well as white/light mineral oils. Mineral oil is believed to have a low toxicity if it is “white,” meaning that all unsaturated and aromatic hydrocarbons have been removed, and if the molecular mass is high enough (average molecular mass higher than 480 Dalton, and less than 5% should be below n-C_{25}), that uptake and subsequent accumulation in human tissue is negligible [3]. In the food industry, petrolatum and mineral waxes are used, for example, as fruit coatings and additives in food packaging, and mineral oils are used as glazing agents, lubricants in food processing machinery, and release agents for baking. A study carried out in the United States estimated the total exposure of mineral hydrocarbons from direct (intentionally added to food) and in-direct (migration from food-contact materials) food-use to be 0.875 mg/kg bw/day [25]. 49% of this estimate was from mineral oil exposure, 46% from petrolatum, and 5% from paraffin and microcrystalline waxes. Direct food applications contributed 99% of the total exposure whereas in-direct exposure from migration into foods accounted for only 1%. A study in Europe gave similar estimates, of which mineral oil exposure was between 0.09-0.91 mg/kg bw/day, and exposure to mineral waxes between 0.01-0.19 mg/kg bw/day [26]. These findings were not alarming at the time, seeing as the exposure estimates were far less than the acceptable daily intake (ADI) as determined by the Scientific Committee for Food. The ADI limits were 20 mg/kg bw/day for microcrystalline waxes,

and 4 mg/kg bw/day for certain white mineral oils at the time [26]. Table 2.2 gives the most recently updated ADI as determined by the joint FAO/WHO Expert Committee on Food Additives (JECFA) and the Scientific Committee for Food (SCF).

Table 2.2: Acceptable daily intake of different classes of mineral oils [1, 3]

		Carbon number at 5% distillation point	**Average molecular mass [Da]**	**ADI [mg/kg bw]**
High viscosity oils		>28	>500	0–20
Medium and low viscosity oils	Class I	>25	480–500	10
	Class II	22	400–480	0.01
	Class III	17	300–400	0.01

2.3.1.2 MOSH and MOAH

It has been found that mineral oils not intended for food contact applications eventually were able to reach the food chain by ways of migration from jute or sisal bags [27] and printing inks [28] into the foods. These foods contained a technical grade of mineral oil hydrocarbons not intended for food-use, and most concerning was the presence of mineral aromatics found in the food. Technical grades of mineral oils are generally used for motor or engine oils, and hydraulic oils. Moret et al. identified the source of contamination as the batching oil used to treat jute or sisal fibres before the spinning process, which is a crude mineral oil that usually has a brown colour [27]. Droz and Grob showed that the mineral oils used as a diluent in printing inks for cardboard boxes were transferred to the food even if the food were packed in an additional unprinted paper bag [28]. Since these findings, it became evident that a more detailed characterisation of mineral hydrocarbons, as well as appropriate regulations, was required in order to protect consumers.

Biedermann et al. [29] used the terms “mineral oil saturated hydrocarbons” (MOSH) and “mineral oil aromatic hydrocarbons” (MOAH) to distinguish between the two types of compounds. MOSH refers to paraffins (straight chain and branched hydrocarbons) and naphthenes (cyclic saturated hydrocarbons), but it excludes the hydrocarbons that are naturally present in foods, such as the n-alkanes from plant origin. MOAH is the aromatic hydrocarbons from mineral origin, and it differs from

the polyaromatic hydrocarbons (PAHs) in that they are highly alkylated as opposed to PAHs that consists of mostly nonalkylated rings.

2.3.2 Sources of contamination

Mineral oils used in the manufacturing of jute bags have been found to contaminate foods transported and stored in these bags [27]. In 1997, it has been established that dry foods packaged in cardboard boxes were contaminated by mineral oils [28]. As a result, the packaging was tested as a possible source of contamination, and it was found that the mineral oils were present only in printed cardboard boxes, and not in unprinted boxes. Exposure of uncontaminated food to ink vapours proved that mineral oils ranging from C_{14} to C_{22} migrated into the food via the gas phase [28]. Mineral oils found in recovered fibre originate mainly from solvents present in printing inks used in the newsprint (offset printing), waxes used to improve the water resistance of paperboard, components in adhesives, diluents for binders, and inks from offset printing for decorative printing on cartons. Offset printing inks are available as either cold-set or heat-set inks, differing in their composition of pigment, resin, and mineral oil vehicle. Cold-set inks contain about 60 wt % mineral oils, whereas heat-set inks contain about 24–40 wt % [30]. Newspapers are usually printed with the cold-set type of printing, which uses no heat to dry the ink, but rather dries by absorption into the paper, and evaporation into air, and can be easily recognised by the ink rub off visible on your hands. When these inks make their way back into the recycling system, they are often incorporated into paperboard used for food packaging, which then finally contains quantities of non-food grade mineral oils. In addition to packaging containing recycled newsprint, some inks used for printing paperboard contain mineral oil solvents, and can thus also act as a source of contamination when these cartons are used for food packaging [1, 28].

2.3.3 Mineral oil migration

Biedermann et al. [1] showed that the MOSH and MOAH content in newsprint was only evident in the printed regions, and thus concluded that ink is the main reason for high mineral oil ($<C_{28}$) content up to 300-1000 mg/kg in recycled board. They also showed that mineral oils up to C_{24} migrated readily to the food and up to C_{28} to a lesser extent. The reason for this is that migration of these hydrocarbons into foodstuff occurs via the vapour phase [28], hence the ability to migrate remains proportional to their partial vapour pressure. These tests were limited in terms of determining the total mineral oil migration at the expiry date, as mineral oil migration studies have only been carried out on food and board samples that have been stored under appropriate conditions for lengthy periods of time, or

taken from the shelf before the expiry date of the product shelf-life. The total migration potential was thus estimated by assuming that 70% of all mineral oils up to n-C_{24} present in the paperboard will somehow migrate into foodstuffs [2]. However, this assumption does not take into account novel strategies proposed to prevent mineral oil migration, such as the use of a functional barrier between the mineral-oil-containing packaging and the foodstuff. In these cases, actual migration studies need to be carried out in order to measure the actual capability of mineral oil to migrate from the packaging into foodstuff through a barrier material. Such tests could take from a few months to up to years, to determine the actual migration potential under real conditions of use.

2.4 Migration studies into food

The SML for contaminants in packaging materials are usually given as mg substance per kg of food. This concentration limit in food can be converted to the contaminant concentration in the paperboard, based on the assumption that generally 6dm^2 of packaging is required to pack 1kg of food [11], therefore:

$$SML\frac{[mg]}{[kg\ \ food]}\times\frac{1\,[kg\ \ food]}{6\,[dm^2\ \ paper]}=0.1\dot{6}\cdot SML\frac{[mg]}{[dm^2\ \ paper]}=Q_a \qquad \textbf{Eq. 2.1}$$

In the same way, the OML of 60 mg/kg food thus corresponds to 10 mg/dm^2 paper. This concentration based on packaging area, Q_a, could be converted to restriction limits by mass of packaging analysed, by using the grammage (mass per unit area) of the paperboard:

$$Q_m=\frac{Q_a\cdot 100\,000}{G} \qquad \textbf{Eq. 2.2}$$

where Q_m is the concentration of contaminant in the paper in mg/kg, G is the grammage in g/m^2, and Q_a is the concentration of contaminant in paper in mg/dm^2. Q_m is the maximum quantity of the contaminant allowed in the packaging, if it is assumed that 100% will migrate into the foodstuff.

2.4.1 Mechanisms of migration

Migration of undesirable chemicals from packaging materials into foodstuff can be categorised into two types, namely leaching or volatile mechanisms [31].

Leaching migration requires intimate contact between the packaging and the food, such as typically the case with liquid foodstuffs. In leaching systems, the migrant generally has a high diffusion coefficient in the packaging, and can be readily dissolved in the contacting food phase. The migration process involves three steps: (1) diffusion of migrant in the packaging wall towards the food-packaging interface; (2) dissolution of migrant at the food-packaging interface; and (3) dispersion of the migrant into the food.

Volatile systems do not necessarily require contact between the food and the packaging, as is the case with dry solid foods with poor direct contact with the package walls. Migration to the food can occur with volatile compounds that have relatively high vapour pressures at room temperature. This migration process includes: (1) diffusion of migrant in the packaging wall towards the food-packaging interface; (2) desorption of migrant at the food-packaging interface; and (3) adsorption of volatile compounds from the headspace onto the food. The migration phenomenon is, in most cases, controlled by the diffusion in the packaging material (or the diffusion coefficient of the migrant), rather than the characteristics of the food phase.

2.4.2 Migration testing

Migration of chemical substances is a diffusion process that is controlled by kinetic and thermodynamic activities. With the onset of migration, a concentration gradient due to diffusion commences in the packaging substrate, after which the concentration of the migrant in the food starts to increase, until equilibrium is reached between these two phases and no more concentration gradient exists in the packaging [31]. During the migration process, at the interface between the packaging and food, the relationship between the concentration of the migrant in the packaging and that in the food, is governed by a partition coefficient, $K_{p/f}$ described by equation 2.3:

$$K_{p/f} = \frac{C_{p,\infty}}{C_{f,\infty}} \qquad \textbf{Eq. 2.3}$$

where $C_{p,\infty}$ and $C_{f,\infty}$ are the concentrations (measured in $mg.m^{-3}$) in the packaging and the food at infinite contact time, respectively. Therefore, the amount of migration depends on the diffusion coefficient of the potential migrant in the packaging, but also its partition coefficient into the food. Figure 2.1 shows the effect of both these parameters on the migration process. Higher diffusion

coefficients result in a faster approach to equilibrium, whereas higher partition coefficients influence the final level of migration at equilibrium. $K_{p/f}$ depends on the polarity and solubility of migrant in the food.

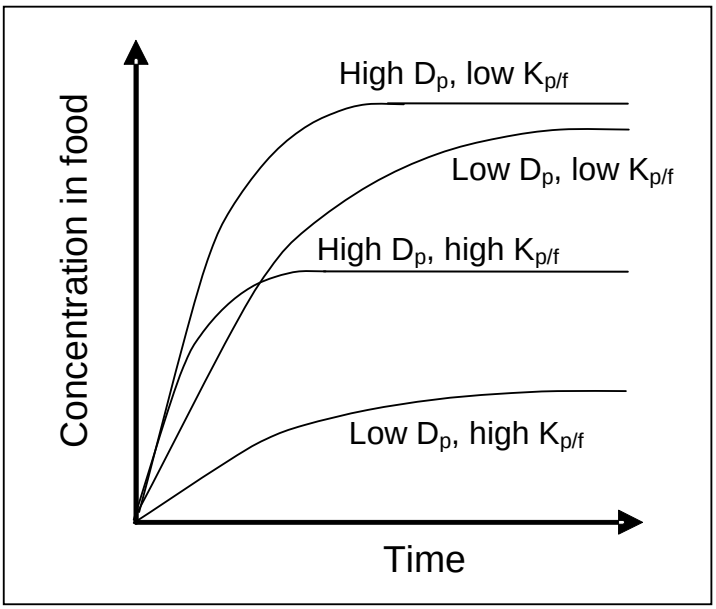

Figure 2.1: Concentration of a migrant into foodstuff over time [31].

2.4.2.1 Deliberate dosing of paper with surrogate compounds

Impregnation of paper samples with surrogate chemicals was a common procedure in order to develop proper test methods for migration studies, as concentrations of contaminants are extremely low (ppb range, and sometimes ppm range). Song et al. selected five model surrogate compounds to represent five different categories of contaminants [32]. These were anthracene, representing polyaromatic hydrocarbons (PAHs); benzophenone, representing photoinitiators in UV-curable inks; dimethyl phthalate, representing adhesives; methyl stearate, representing defoamers; and pentachlorophenol, representing biocides. Triantafyllou et al. selected a couple of model compounds which were suspected to be present in recycled paper and board packaging. These included *o*-xylene, acetophenone, benzoic acid, dodecane, naphthalene, vanillin, diphenyl oxide, 2,3,4-trichloroanisole, benzophenone, DIPN, dibutyl phthalate (DBP), and methyl stearate [13, 20, 21]. The paper samples were dosed with known concentrations of the surrogate compounds, which were then placed in a closed vial together with dry food. Elevated temperatures (70 and 100 ℃) were utilised to speed up the migration process. A migration equilibrium was reached within as short as 1 hour, and it was found that the % of migration was dependant on the volatility of the contaminants.

2.4.2.2 Migration into food simulants

Since actual foodstuff is quite complex to analyse for migration of contaminants from the packaging to the food itself, it was found to be satisfactory to use a food simulant. This provided the advantage that results are more consistent and reliable, due to the more simple and known composition of a food simulant as compared to actual food [31]. Food simulants can be liquid or solid substances with similar contaminant extraction capacity to the foodstuffs. The European Commission gives clear regulations with regards to test methods for materials to come into contact with food. Commission Regulation (EU) No. 10/2011 [33] on plastic materials and articles intended to come into contact with food, gives a list of food simulants representing different groups of foodstuff, that may be used in migration testing. Information about simulants for different types of food is summarised in Table 2.3.

Table 2.3: Food simulants and their corresponding food types [33]

Food simulant	Abbreviation	Applications
10% (v/v) Ethanol	A	Aqueous food if the pH value of the foodstuff is > 4.5 Alcoholic food with alcoholic strength < 10%
3% (w/v) Acetic acid	B	Acidic foods, if the pH value of the foodstuff is < 4.5
20% (v/v) Ethanol	C	Alcoholic foods containing up to 20% alcohol
50% (v/v) Ethanol	D1	Dairy products, foods with alcoholic strength >20%
Vegetable oil	D2	Fatty foods
Poly(2,6-diphenyl)-*p*-phenylene oxide [Tenax®]	E	Dry foods

Recycled paper in direct contact with food is mainly used for packaging of dry foods, such as flour, sugar, rice, and pasta. These foods usually have a relatively high surface area, and are thus the most affected by mineral oil migration. Modified polyphenylene oxide, under the trademark name Tenax, is a proper simulant for dry foods with a low to intermediate fat content [13, 21]. It was found that foods with higher fat contents (e.g. infant whole milk powder with a fat content of >27%) demonstrated a higher migration tendency of volatile organic compounds than that found with Tenax. Tenax is a porous polymer material with the ability to trap volatile compounds, has a high sorption capacity, high thermal stability, high purity, and consistent quality. The European standard EN 14338:2003 is a test method for measuring the migration of volatile and semi-volatile substances from paper and board into this food simulant [34].

2.4.2.3 Accelerated measurements

The kinetics of migration of model contaminants, with boiling points between 144–442℃, from recycled paperboard samples showed that an equilibrium migration was achieved in a couple of hours at elevated temperatures [21]. Aurela et al. [5] has shown that a 4 month storage period of sugar gave similar phthalate migration results to accelerated measurements for 10 days at 40℃, with Tenax as food simulant.

EN 1186-1:2002 [35], annex B, as well as Commission Directive 97/48/EC [36] and Annex 1 of Directive 2002/72/EC [37] gives the conditions of testing, such as time and temperatures for different migration tests in order to find the most suitable accelerated conditions to correspond to the potential real-life conditions of the product. However, Commission Regulation (EU) No. 10/2011 on plastic materials and articles intended to come into contact with food, provides updated details on accelerated testing conditions in terms of real conditions of use, i.e. conditions for frozen foods varies from that of long term storage at room temperature, for instance. Table 2.4 gives the details of the contact conditions, time and temperature, when using food simulants in migration experiments.

Table 2.4: Contact conditions for migration testing with food simulants [33]

Contact time		**Contact temperature (℃)**	
Actual contact time between food and packaging	Test time for accelerated measurements	Actual contact temperature	Test temperature for accelerated measurements
t ≤ 5 min	5 min	T ≤ 5 ℃	5 ℃
5 min < t ≤ 30 min	30 min	5 ℃ < T ≤ 20 ℃	20 ℃
30 min < t ≤ 1 h	1 h	20 ℃ < T ≤ 40 ℃	40 ℃
1 h < t ≤ 2 h	2 h	40 ℃ < T ≤ 70 ℃	70 ℃
2 h < t ≤ 6 h	6 h	70 ℃ < T ≤ 100 ℃	100 ℃
6 h < t ≤ 24 h	24 h	100 ℃ < T ≤ 121 ℃	121 ℃
1 day < t ≤ 3 days	3 days	121 ℃ < T ≤ 130 ℃	130 ℃
3 days < t ≤ 30 days	10 days	130 ℃ < T ≤ 150 ℃	150 ℃
t > 30 days	See Eq. 2.4	150 ℃ < T < 175 ℃	175 ℃
		T > 175	Real temperature

It should be noted that simulants A, B, C, and D1 can not be used at temperatures higher than 100℃. When temperature conditions higher than 100℃ are r equired, the test temperature should be 100℃ or a reflux temperature, but the time should be adjusted to 4 times that of the selected test time conditions. In addition, for long term storage conditions of more than 30 days at room temperature or below, the following formula were derived to determine the test time:

$$t_2 = t_1 \times e^{\left(-\frac{E_a}{R}\right)\left(\frac{1}{T_1}-\frac{1}{T_2}\right)} \qquad \textbf{Eq. 2.4}$$

where t_1 is the actual contact time; t_2 is the testing time; E_a is the worst case activation energy of 80 kJ.mol^{-1}; R is a factor of 8.31 J/K/mol; T_1 (in Kelvin) is the actual contact temperature; and T_2 (in Kelvin) is the test temperature as determined from Table 2.4.

2.4.2.4 Analytical techniques

The OML, as previously reported to be 60 mg/kg food, is most commonly measured gravimetically. In such a case, the difference in weight before and after the migration test, gives the overall migration. Other less conventional analytical techniques involve measuring the change in optical density of a liquid simulant, $KMnO_4$ titration of organic extractables in distilled water, or sensorial testing (smell or taste) which is only qualitative.

Certain food contact substances face an SML according to mandatory regulations. In this case, the analytical technique for quantifying the specific migration should be the most appropriate technique for that particular substance. These analyses commonly involve FT-IR, GC-MS, or HPLC-MS, usually preceded by an enrichment step due to very low concentrations [31].

2.5 Analytical identification and characterization of mineral oils

Mineral hydrocarbons are most commonly analysed by on-line coupled liquid chromatography and capillary gas chromatography (LC-GC) [28, 38-40]. FID is the detector of choice for hydrocarbons. In the case of food analysis, Droz and Grob [28] used liquid chromatography (LC) pre-separation with a silica column to separate naturally occurring oils in food from the mineral oil hydrocarbons. GC, equipped with a flame ionization detector (FID), was then used to separate the mineral oil hydrocarbons according to carbon number. This presented the mineral oil hydrocarbons as a broad hump of unresolved material, topped by n-alkane peaks. Even though MOSH were not separated from MOAH, the broad hump indicated that over 98% of the mineral oils had a branched or cyclic structure, and the total mineral oil content in food was successfully quantified [28]. However, in the case of gasoline and diesel samples, the LC stage has been used to separate mineral hydrocarbon groups such as saturates, unsaturates, aromatics, and polar compounds. GC-FID allowed separation of the different groups according to carbon number [39].

Walters et al. [24] used quantitative FT-IR to determine the amount of mineral hydrocarbons in food. However, this technique has the limitation that hydrocarbons are quantified as a group, as it cannot distinguish between the different types of hydrocarbons. Grob [41], Wagner [42], and Populin [43] et al. utilised two-dimensional liquid chromatography involving two silica gel columns, the first to separate fats and edible oils from hydrocarbons, and the second to separate saturated mineral hydrocarbons, from unsaturated hydrocarbons naturally occurring in food oils or fats. However, saturated n-alkanes are also present in natural products, but these are usually recognised by the predominant odd-numbered carbon atoms (larger peak sizes compared to that of even-numbered paraffins), and can thus be distinguished from mineral origins. However, this method takes into consideration the presence of MOSH only, and MOAH is thus not included in the quantification of mineral oil contamination of food. Fiselier et al. [44] showed a method for removing the long chain n-alkanes originating from plants by using activated aluminium oxide and in doing so improved analysis of MOSH.

Moret et al. [45] described a method using two-step liquid chromatography with intermediate solvent evaporation (SE), and automatic transfer to GC-FID, i.e. LC-SE-LC-GC-FID, by which mineral hydrocarbons are separated from food extracts such as fats and edible oils in the first silica gel

column, and paraffins are separated from aromatics in the second aminosilane column. MOAH was separated according to ring-number, and GC-FID enabled the identification and quantification of paraffins according to carbon-number, and of aromatics according to ring-number [27]. Because MOSH and MOAH consist of extremely complex mixtures, GC-FID forms broad humps of unresolved compounds. But this is still the preferred method of choice as GC allows characterization of MOSH and MOAH, given that these two groups were preseparated. Furthermore, GC also allows distinction from hydrocarbons naturally present in foods, while FID is the only system giving more or less the same response for all aromatic hydrocarbons (regardless of alkylation) [29]. Biedermann et al. [1, 29] developed a simple method for quantifying both MOSH and MOAH. They used normal phase HPLC and transferred on-line to GC-FID, but this was preceded by epoxidation for removal of polyolefins naturally present in foods and edible oils, and an enrichment stage for removal of lipids in order to reach the detection limit. MOAH was quantified as a group, and characterization according to ring-number was achieved with two-dimensional GC. Both groups, MOSH and MOAH, gave peaks on top of large humps of unresolved compounds from HPLC-GC-FID results; MOSH due to the presence of isoparaffins (branched) and cycloparaffins; and MOAH due to differences in alkylation on the same ring number.

Because MOSH and MOAH consist of extremely complex mixtures, it is generally not possible to obtain suitable standards for calibration purposes. For this reason, GC-FID still remains the method of choice for mineral hydrocarbon analysis; GC for its capability of separating hydrocarbons according to molecular mass, and FID since the response for a certain amount of paraffins is in effect independent of the composition [29]. MOSH and MOAH can, therefore, be characterised and quantified separately only once these two groups have been pre-separated. It is clear that mineral oil contaminants in paper packaging and foodstuffs are quite complex, and subsequently requires expensive equipment as well as highly skilled operators for proper assessment. For this reason, one of the objectives of this study is to develop a simplified test method that will allow papermakers to evaluate the ability of paperboard to protect foodstuff against cross-contamination via the vapour phase by mineral oil and other volatile organic contaminants from primary, secondary or even tertiary packaging.

2.6 Strategies to prevent mineral oil migration

The BfR Forum discussed several possibilities to minimise or prevent the migration of mineral oils from paper packaging into the food, however, these are not solutions achievable at once. Substituting recycled board packaging by virgin board is economically and environmentally not viable. Selection of starting materials with a low mineral oil content may be difficult, as recovered fibres are often mixed and from unknown sources. It is believed that only 0.23 wt % newspaper in the recovered fibre mixture can cause the current recommended limit for MOSH to be reached in the final product [46]. The recycling process could be optimised in such a way that mineral oil compounds are removed more efficiently, even though it is believed that this will not solve the problem entirely. Substitution of mineral oil-based inks used in the newsprint industry by food grade oils would also require time and heavy investment by printers, making this option difficult to implement in the short to medium term.

One of the most favoured solutions is to protect the foodstuff with a proper barrier. Inner liner bags could act as a barrier to migration if an impermeable material such as aluminium is used. When internal bags were used between the food and paper packaging, it was found that aluminium, polyethylene terephthalate (PET), and acrylate-coated PP bags acted as good barriers to mineral oil migration into food [2]. In addition, the BfR proposed that impermeable paper coatings could also be a possible solution, as this may also prevent the migration of other volatile organic compounds (VOCs) contaminating the food.

In this study, we propose the use of coated polymeric films on paperboard as barriers to mineral oil migration. The use of waterborne polymers is not only environmentally friendly, but also allows future recyclability or repulpability, as compared to laminate films. A large variety of commercially available lattices are able to provide excellent barriers against, for example, grease, oxygen or aroma that might be effective for mineral oil as well.

2.7 Gas and vapour transport through polymer films

The subject on transport of gases and vapours through polymeric membranes has been studied since the 19th century. The solution-diffusion model is a widely accepted model which describes the transport of a penetrant across a matrix, from a high pressure region to a low pressure region, and consists of the following steps (see Scheme 2.1) [47]:

- Absorption of the penetrant on the matrix surface exposed to higher partial pressure (upstream side);
- Diffusion of the penetrant inside the matrix under a concentration gradient;
- Desorption of the penetrant from the matrix surface at the side of lower partial pressure (downstream side).

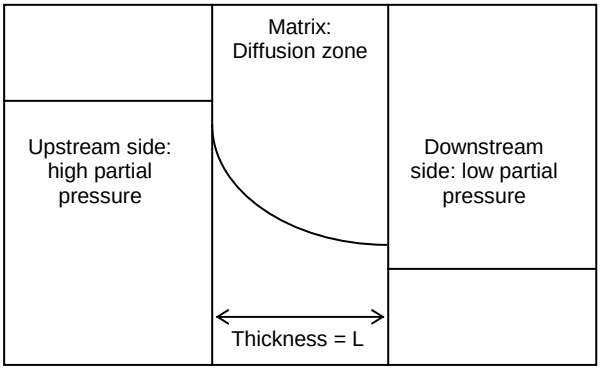

Scheme 2.1: Three steps of the transport principle [47]**.**

2.7.1 Permeability

Generally, permeability can be defined as the steady state transport of a penetrant across a polymer membrane, which is quantified by applying *Fick's law of diffusion* and *Henry's law of solubility*, i.e. the permeability coefficient (P) is the product of the diffusion coefficient (D) and the solubility coefficient (S) [48]:

$$P = D \times S \qquad \textbf{Eq. 2.5}$$

The permeability coefficient illustrates the ease with which a penetrant will move through a matrix when it is applied to a pressure gradient. The diffusion coefficient is a kinetic term that describes the mobility of the penetrant in the matrix, and the solubility coefficient is a thermodynamic term that gives an indication of the interaction between the penetrant and the matrix [47]. Therefore, the permeability coefficient depends on the nature of the penetrant, nature of the polymer matrix, the pressure gradient of the penetrant across the matrix and the temperature.

2.7.2 Solubility

The solubility coefficient is a result of the interactions between polymer and penetrant. The solubility coefficient is generally a function of temperature, pressure, or concentration [47].

2.7.3 Diffusion

Diffusion can be described as the process by which a small penetrant molecule is transferred through a matrix due to random molecular motions [47]. Gases have a natural tendency to diffuse from areas of high concentration, or high chemical potential, to areas of low concentration, or low chemical potential, until a state of equilibrium is reached where no concentration gradient exists, i.e. constant chemical potential [49]. The kinetics of diffusion refers to the relative mass uptake as a function of time, at a specific/given penetrant partial pressure, and is illustrated by equation 2.6:

$$\frac{M_t}{M_\infty} = kt^n \qquad \textbf{Eq. 2.6}$$

where M_t is the mass of penetrant uptake at time *t* and M_∞ is the mass uptake at equilibrium, *k* is a constant and *n* is an indication of the type of diffusion mechanism.

2.7.3.1 Diffusion mechanisms

Generally, two different types of diffusion mechanisms exist, namely Fickian and non-Fickian behaviour (sorption and permeation kinetics). In the case of Fickian behaviour (where *n* = 0.5, see equation 2.6 and Figure 2.2), polymer chains relaxation time is greater than the rate of diffusion of the penetrant. This is the ideal case of penetrant transport, since diffusion of penetrant is followed by immediate response of the polymer chains, thus allowing the system to rapidly reach the sorption equilibrium.

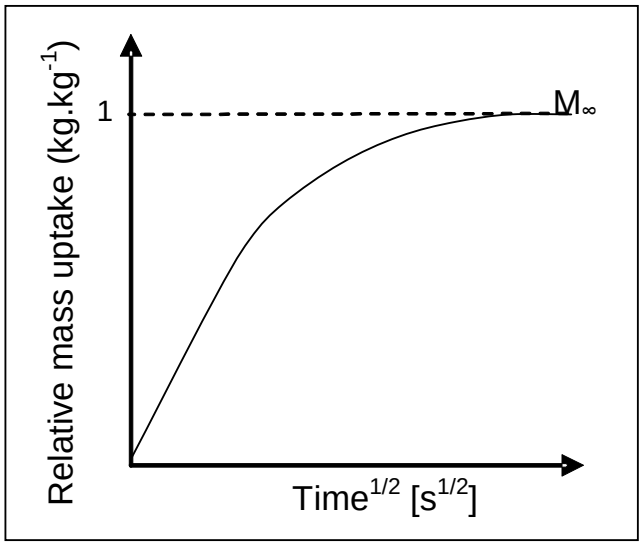

Figure 2.2: Fickian diffusion: M_t/M_∞ **vs.** $\sqrt{time}$ [50]**.**

Non-Fickian behaviour occurs when anomalous curves are obtained compared to the ideal Fickian behaviour ($0.5 \leq n \leq 1$). These non-Fickian behaviours are typically classified according to the appearance of the kinetic plot, such as two-stage, sigmoidal (S-shaped), and Case II sorption.

2.7.4 Determination of the transport coefficients

The quantification of diffusion of gases/vapours through polymer films can be carried out in two ways, namely permeation and sorption. The difference between these two methods is demonstrated by the presence (permeation) or absence (sorption) of a gas/vapour pressure gradient on either side of the polymer film, as shown in Scheme 2.2.

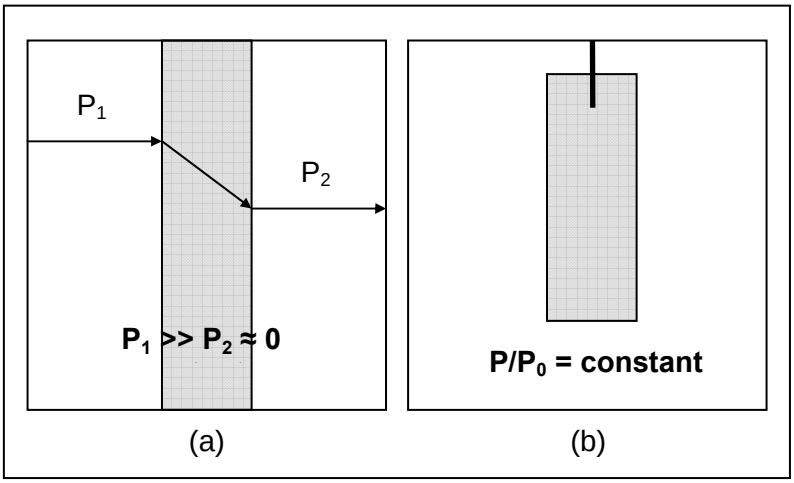

Scheme 2.2: (a) Permeation and (b) sorption experiments.

2.7.4.1 Permeation

In permeation experiments the two sides of a membrane are sealed off from one another, and a penetrant is introduced on the upstream side. This experiment measures the rate of transport of a penetrant from a region of high pressure (p_1), across a membrane, to a region of low pressure (p_2) [48]. The pressure at the two surfaces of the membrane remains constant, and $p_1 >> p_2$. This pressure gradient is the driving force for penetrant flow through the membrane from high partial pressure to low partial pressure. A typical permeation curve is shown in Figure 2.3, where the concentration of the penetrant, Q(t), is plotted as a function of time, *t*.

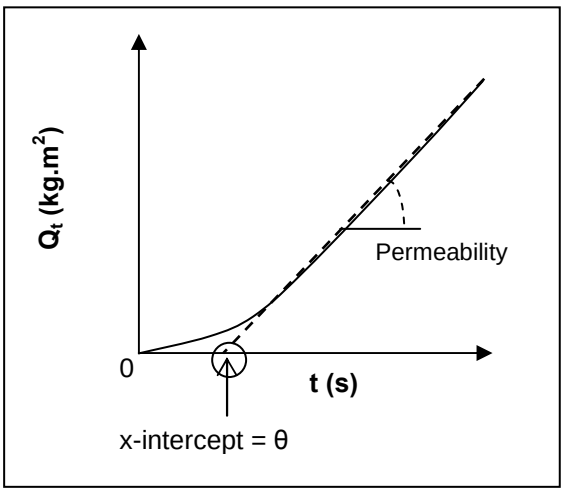

Figure 2.3: A typical permeation curve [48, 50, 51]**.**

Initially, when the penetrant is revealed to the one side of the membrane, the flow and concentration of penetrant, at any point in the membrane, varies as a function of time. This is known as the time lag period. However, once a constant penetrant concentration is reached throughout the thickness of the film, as *t* tends towards longer times, is the steady state reached. During steady state conditions the diffusion of penetrant through the membrane remains constant, or independent of time, as shown by the straight line segment in Figure 2.3.

In these permeation experiments, the diffusion coefficient can be calculated via the time lag method, which means that the intercept between the straight line in Figure 2.3, and the *x*-axis is equal to:

$$\theta = \frac{L^2}{6D} \qquad \textbf{Eq. 2.7}$$

where θ is the time lag (measured in seconds), and L is the thickness of the substrate (measured in centimetres). Therefore, the diffusion coefficient, D, with units cm^2/s, can be calculated. The slope of the steady state conditions is equal to the permeability, P, with units cm^3(STP).cm/s.cm^2(cmHg).

Once the steady state conditions are reached, P can be calculated from the slope of the permeation curve (Figure 2.3), since [52]:

$$P = \frac{\Delta Q.L}{\Delta t.A.p_1} \qquad \textbf{Eq. 2.8}$$

2.7.4.2 Sorption

The sorption method means that the penetrant activity at both sides of the polymer film is the same as the film is being immersed into the penetrant vapours. This allows for a continuous mass uptake of penetrant by the polymer film, until a state of equilibrium is reached after a period of time, when the polymer film becomes saturated with penetrant. The data from a sorption experiment are usually presented as the amount, in grams, of gas/vapour absorbed or desorbed as a function of the square root of time, i.e. $M_t = f(t^{1/2})$, and this is known as the sorption curve. After a certain amount of time, the sorption eventually reaches equilibrium, at which the membrane no longer absorbs or desorbs any of the diffusing molecules, and therefore M_t reaches M_∞. It is, however, more convenient to plot M_t/M_∞ against $t^{1/2}/L$, where L is the thickness of the membrane (see Figure 2.4), and is known as the reduced sorption curve. This type of plot has the advantage that sorption data of membranes with different thicknesses are comparable and can be overlayed in the same graph.

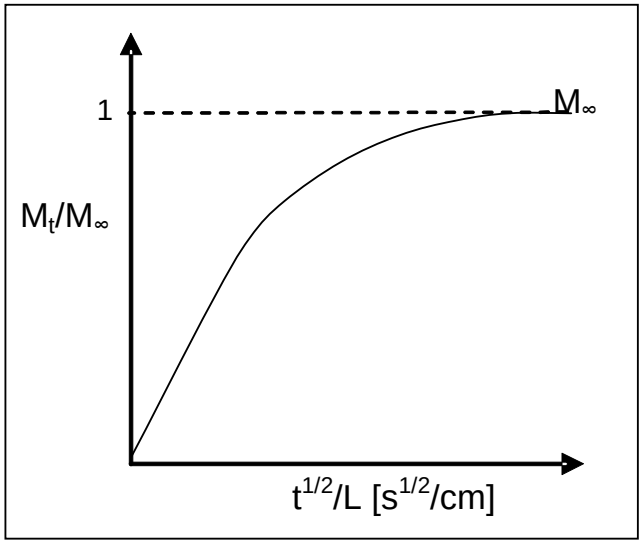

Figure 2.4: Reduced sorption curve [48]**.**

The transport coefficients D and S can also be determined from the reduced sorption curve. After a given amount of time, at constant D, temperature, and pressure, the amount of penetrant absorbed by the membrane is given as [51]:

$$\frac{M_t}{M_\infty} = 1 - \sum_{n=0}^{\infty} \frac{8}{(2n+1)^2 \pi^2} \exp\left[\frac{-D(2n+1)^2 \pi^2 t}{L^2}\right] \qquad \textbf{Eq. 2.9}$$

The solubility coefficient is derived from the volume of gas absorbed at equilibrium sorption, V_∞, measured in cm^3, in standard temperature and pressure (STP) conditions:

$$V_\infty = \frac{M_\infty - M_i}{M_g} 22\,400 \qquad \textbf{Eq. 2.10}$$

where M_i is the initial mass of the sample, M_g is the molar mass of the gas/vapour, and the constant 22 400 corresponds to the volume (cm^3) occupied by 1 mole of gas/vapour in STP conditions. Using this value, S is obtained by equation 2.11:

$$S = \frac{V_\infty}{p V_{pol}} \qquad \textbf{Eq. 2.11}$$

where p is the pressure of the gas/vapour, and V_{pol} is the volume of the polymer membrane.

In the absence of complicating polymer relaxation rate behaviour (Fickian sorption), plots such as those in Figure 2.4 are typically linear from origin up to at least 50% of the total change in penetrant concentration [52]. At some point above 50%, the curve becomes concave to the time axis. Therefore,

a halftime can be defined, t = $t_{1/2}$, where the ratio of M_t/M_∞ is equal to ½, and the diffusion coefficient could be derived from equation 2.9, and is given as:

$$D = \frac{0.04919}{\left(\frac{t}{L^2}\right)_{1/2}} \qquad \textbf{Eq. 2.12}$$

2.7.4.3 Sorption isotherms [47]

Sorption experiments can be carried out at different penetrant activities, i.e. partial pressure of the penetrant. The relationship between the penetrant uptake as a function of partial pressure, under constant temperature conditions, therefore describes the sorption isotherm. Diffusing molecules may be sorbed according to different sorption modes, even in the same polymer membrane. These sorption modes are determined by the thermodynamics of the polymer-penetrant interactions. The different isotherm plots of penetrant concentration vs. vapour pressure are shown in Figure 2.5.

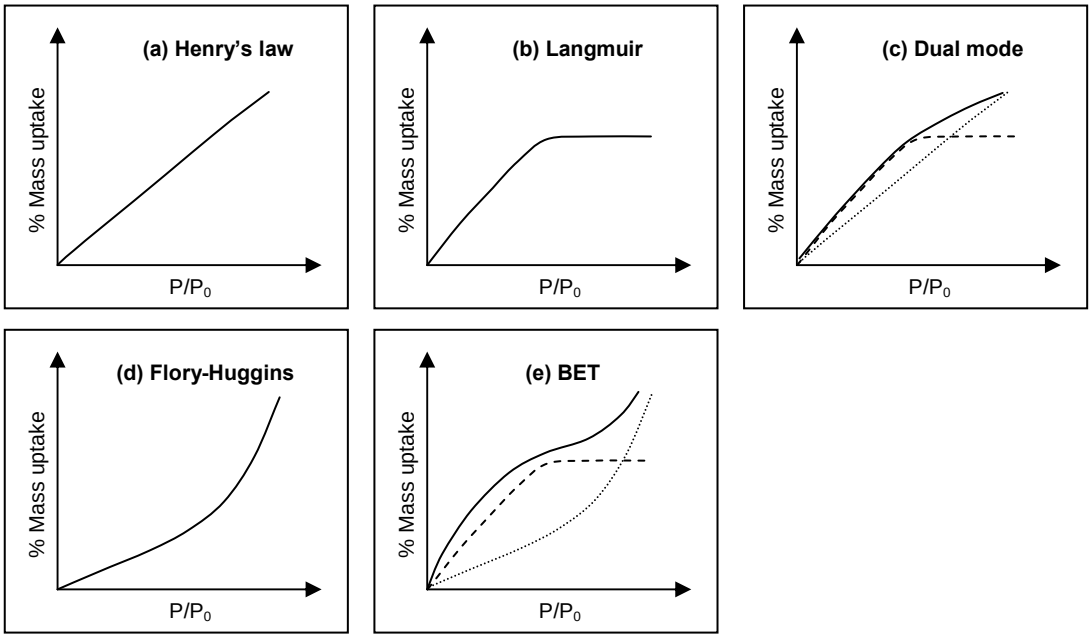

Figure 2.5: Sorption isotherms [50]**.**

Henry's law sorption isotherms: Figure 2.5 (a) shows the ideal sorption isotherm, where a linear relationship exists between the penetrant concentration and the partial pressure. In this case, there are no polymer-penetrant, or penetrant-penetrant interactions, and are generally observed with ideal gases. This usually occurs at low pressures where the polymer-polymer interactions dominate, the solubility coefficient is constant, and therefore Henry's Law is obeyed.

Langmuir-mode sorption isotherms: This mode of sorption usually occurs with polymers containing microvoids or inorganic fillers, whereby penetrant molecules can occupy specific sites in the polymer matrix. Therefore, polymer-penetrant interactions dominate in this mode of sorption. When all these sites are occupied, a small quantity of diffusing molecules may solubilise, and the typical isotherm plot is given in Figure 2.5 (b).

Dual-mode sorption isotherms: This model suggests the existence of two distinct populations of diffusing molecules, namely molecules dissolved in the polymer matrix of which the concentration follows Henry's law; and molecules trapped in specific sites in the polymer matrix or which the concentration follows the Langmuir model (see Figure 2.5 [c]). This dual mode can be used to describe the sorption of low activity gases in glassy polymers. It is only valid for moderate pressures in the absence of strong interactions, and when there is no swelling or plasticising effects caused by the sorbed molecules on the polymer matrix.

Flory-Huggins sorption isotherms: Figure 2.5 (d) shows a continuous increase of the solubility coefficient with pressure. The reason for this effect is since the interactions between the diffusing molecules are much stronger (penetrant-penetrant interactions) than the penetrant-polymer interactions. This may be the result of either a plasticising effect of the polymer by the sorbed molecules, or the association of clusters for example in the case of water-hydrophobic polymer systems.

BET sorption isotherms: The Brunauer, Emmett and Teller (BET) model describes a combination of the Langmuir and Flory-Huggins sorption modes, as illustrated in Figure 2.5 (e). It is characteristic of the sorption of water vapour by highly hydrophilic polymers, where firstly the water molecules are strongly sorbed in specific sites such as polar groups, characterised by the initial concave shape of the isotherm. Secondly, cluster associations may occur at higher pressures, which lead to the convex shape in the sorption isotherm.

References

1. Biedermann, M. and Grob, K., Is recycled newspaper suitable for food contact materials? Technical grade mineral oils from printing inks. *Eur. Food Res. Technol.,* (2010) 230: 785–796.
2. Vollmer, A., Biedermann, M., Grundbock, F., Ingenhoff, J.-E., Biedermann-Brem, S., Altkofer, W., and Grob, K., Migration of mineral oil from printed paperboard into dry foods: survey of the German market. *Eur. Food Res. Technol.,* (2011) 232: 175–182.
3. Scotter, M. J., Castle, L., Massey, R. C., Brantom, P. G., and Cunninghame, M. E., A study of the toxicity of five mineral hydrocarbon waxes and oils in the F344 rat, with histological examination and tissue-specific chemical characterisation of accumulated hydrocarbon material. *Food Chem. Toxicol.,* (2003) 41: 489–521.
4. Binderup, M.-L., Pedersen, G. A., Vinggaard, A. M., Rasmussen, E. S., Rosenquist, H., and Cederberg, T., Toxicity testing and chemical analyses of recycled fibre-based paper for food contact. *Food Addit. Contam.,* (2002) 19: 13–28.
5. Aurela, B., Kulmala, H., and Soderhjelm, L., Phthalates in paper and board packaging and their migration into Tenax and sugar. *Food Addit. Contam.,* (1999) 16: 571–577.
6. Boccacci-Mariani, M., Chiacchierini, E., and Gesumundo, C., Potential migration of diisopropyl naphthalenes from recycled paperboard packaging into dry foods. *Food Addit. Contam.,* (1999) 16: 207–213.
7. Summerfield, W. and Cooper, I., Investigation of migration from paper and board into food - development of methods for rapid testing. *Food Addit. Contam.,* (2001) 18: 77–88.
8. Vinggaard, A. M., Korner, W., Lund, K. H., Bolz, U., and Petersen, J. H., Identification and quantification of estrogenic compounds in recycled and virgin paper for household use as determined by an in vitro yeast estrogen screen and chemical analysis. *Chem. Res. Toxicol.,* (2000) 13: 1214–1222.
9. Grob, K., Pfenninger, S., Pohl, W., Laso, M., Imhof, D., and Rieger, K., European legal limits for migration from food packaging materials: 1. Food should prevail over simulants; 2. More realistic conversion from concentrations to limits per surface area. PVC cling films in contact with cheese as an example. *Food Control,* (2007) 18: 201–210.
10. *Federal Institute for Risk Assessment - BfR Recommendation XXXVI. Paper and board for food contact*, in *www.bfr.bund.de*.

11. *Industry guideline for the compliance of paper and board materials and articles for food contact*, in http://www.cepi.org. March, 2010.

12. Choi, J. O., Jitsunari, F., Asakawa, F., Park, H. J., and Lee, D. S., Migration of surrogate contaminants in paper and paperboard into water through polyethylene coating layer. *Food Addit. Contam.,* (2002) 19: 1200–1206.

13. Triantafyllou, V. I., Akrida-Demertzi, K., and Demertzis, P. G., Migration studies from recycled paper packaging materials: development of an analytical method for rapid testing. *Anal. Chim. Acta,* (2002) 467: 253–260.

14. Johns, S. M., Jickells, S. M., Read, W. A., and Castle, L., Studies on functional barriers to migration. 3. Migration of benzophenone and model ink components from cartonboard to food during frozen storage and microwave heating. *Packag. Technol. Sci.,* (2000) 13: 99–104.

15. Anderson, W. A. C. and Castle, L., Benzophenone in cartonboard packaging materials and the factors that influence its migration into food. *Food Addit. Contam.,* (2003) 20: 607–618.

16. Feigenbaum, A., Laoubi, S., and Vergnaud, J. M., Kinetics of diffusion of a pollutant from a recycled polymer through a functional barrier: recycling plastics for food packaging. *J. Appl. Polym. Sci.,* (1997) 66: 597–607.

17. Wong, K. O., Leo, L. W., and Seah, H. L., Dietary exposure assessment of infants to bisphenol A from the use of polycarbonate baby milk bottles. *Food Addit. Contam.,* (2005) 22: 280–288.

18. Song, Y. S., Begley, T., Paquette, K., and Komolprasert, V., Effectiveness of polypropylene film as a barrier to migration from recycled paperboard packaging to fatty and high-moisture food. *Food Addit. Contam.,* (2003) 20: 875–883.

19. Jickells, S. M., Poulin, J., Mountfort, K. A., and Fernandez-Ocana, M., Migration of contaminants by gas phase transfer from carton board and corrugated board box secondary packaging into foods. *Food Addit. Contam.,* (2005) 22: 768–782.

20. Triantafyllou, V. I., Akrida-Demertzi, K., and Demertzis, P. G., Determination of partition behavior of organic surrogates between paperboard packaging materials and air. *J. Chromatogr. A,* (2005) 1077: 74–79.

21. Triantafyllou, V. I., Akrida-Demertzi, K., and Demertzis, P. G., A study on the migration of organic pollutants from recycled paperboard packaging materials to solid food matrices. *Food Chem.,* (2007) 101: 1759–1768.

22. Perring, L., Alonso, M.-I., Andrey, D., Bourqui, B., and Zbinden, P., An evaluation of analytical techniques for determination of lead, cadmium, chromium, and mercury in food-packaging materials. *Fresenius J. Anal. Chem.,* (2011) 370: 76–81.

23. *An assessment of heavy metals in packaging: 2009 update*. June 30, 2009, Northeast Recycling Council, Inc: Submitted to: U.S. Environmental Protection Agency.

24. Walters, D. G., Sherrington, K. V., Worrell, N., and Riley, R. A., Formulation and analysis of food-grade mineral hydrocarbons in toxicology studies. *Food Chem. Toxicol.,* (1994) 32: 549–557.

25. Heimbach, J. T., Bodor, A. R., Douglass, J. S., Barraj, L. M., Cohen, S. C., Biles, R. W., and Faust, H. R., Dietary exposures to mineral hydrocarbons from food-use applications in the United States. *Food Chem. Toxicol.,* (2002) 40: 555–571.

26. Tennant, D. R., The usage, occurrence and dietary intakes of white mineral oils and waxes in Europe. *Food Chem. Toxicol.,* (2004) 42: 481–492.

27. Moret, S., Grob, K., and Conte, L. S., Mineral oil polyaromatic hydrocarbons in foods, e.g. from jute bags, by on-line LC-solvent evaporation (SE)-LC-GC-FID. *Z. Lebensm. Unters. Forsch.,* (1997) 204: 241–246.

28. Droz, C. and Grob, K., Determination of food contamination by mineral oil material from printed cardboard using on-line coupled LC-GC-FID. *Z. Lebensm. Unters. Forsch.,* (1997) 205: 239–241.

29. Biedermann, M., Fiselier, K., and Grob, K., Aromatic hydrocarbons of mineral oil origin in foods: method for determining the total concentration and first results. *J. Agr. Food Chem.,* (2009) 57: 8711–8721.

30. Pauck, W. J. and Marsh, W., The role of sodium silicate in the flotation deinking of newsprint at Mondi Merebank. *Tappsa J.,* (2002) 20–25.

31. Lee, D. S., Yam, K. L., and Piergiovanni, L., *Food Packaging Science and Technology*, CRC Press, 2008.

32. Song, Y. S., Park, H. J., and Komolprasert, V., Analytical procedure for quantifying five compounds suspected as possible contaminants in recycled paper/paperboard for food packaging. *J. Agr. Food Chem.,* (2000) 48: 5856–5859.

33. "Commission regulation (EU) No 10/2011 of 14 January 2011 on plastic materials and articles intended to come into contact with food." Official Journal of the European Union.

34. DIN EN 14338 "Conditions for determination of migration from paper and board using modified polyphenylene oxide (MPPO) as a simulant." DEN/TC 172 'Pulp, paper and board'.

35. EN 1186 "Materials and articles in contact with foodstuffs - Plastics - Methods for overall migration." Part 1: Guide to the selection of conditions and test methods for overall migration.

36. "Commission Directive 97/48/EC of 29 July 1997." Official Journal of the European Communities.

37. "Commission Directive 2002/72/EC of 6 August 2002." Official Journal of the European Communities.

38. Micali, G., Lanuzza, F., Curro, P., and Calabro, G., Separation of alkanes in citrus essential oils by on-line coupled high-performance liquid chromatography-highresolution gas chromatography. *J. Chromatogr.,* (1990) 514: 317–324.

39. Apffel, J. A. and McNair, H., Hydrocarbon group-type analyses by on-line multi-dimensional chromatography. *J. Chromatogr.,* (1983) 279: 139–144.

40. Davies, I. L. and Bartle, K. D., On-line fractionation and identification of diesel fuel polycyclic aromatic compounds by two-dimensional microbore high-performance liquid chromatography/capillary gas chromatography. *Anal. Chem.,* (1988) 60: 204–209.

41. Grob, K., Vass, M., Biedermann, M., and Neukom, H.-P., Contamination of animal feed and food from animal origin with mineral oil hydrocarbons. *Food Addit. Contam.,* (2001) 18: 1–10.

42. Wagner, C., Neukom, H.-P., and Grob, K., Mineral paraffins in vegetable oils and refinary by-products for animal feeds. *Mitt. Gebiete Lebensm. Hyg.,* (2001) 92: 499–514.

43. Populin, T., Biedermann, M., Grob, K., Moret, S., and Conte, L., Relative hopane content confirming the mineral origin of hydrocarbons contaminating foods and human milk. *Food Addit. Contam.,* (2004) 21: 893–904.

44. Fiselier, K., Fiorini, D., and Grob, K., Activated aluminum oxide selectively retaining long chain n-alkanes: Part II. Integration into an on-line high performance liquid chromatography–liquid chromatography–gas chromatography–flame ionization detection method to remove plant paraffins for the determination of mineral paraffins in foods and environmental samples. *Anal. Chim. Acta,* (2009) 634: 102–109.

45. Moret, S., Grob, K., and Conte, L. S., On-line high-performance liquid chromatography–solvent evaporation–high-performance liquid chromatography–capillary gas chromatography–flame ionization detection for the analysis of mineral oil polyaromatic hydrocarbons in fatty foods. *J. Chromatogr. A,* (1996) 750: 361–368.

46. Grob, K., History of the case; point of view of an enforcement laboratory. *Intertek MOSH/MOAH Seminar: Migration of mineral oil from packaging materials to foodstuffs*, *22 June 2011*. Amsterdam, Netherlands.

47. Klopffer, M. H. and Flaconneche, B., Transport properties of gases in polymers: bibliographic review. *Oil Gas Sci. Technol.,* (2001) 56: 223–244.

48. Crank, J. and Park, G. S., *Diffusion in Polymers*, Academic Press, London, 1968.

49. Crosby, N. T., *Food packaging materials - aspects of analysis and migration of contaminants*, Applied Science Publishers Ltd., London, 1981.

50. Wel, G. K. v. d. and Adan, O. C. G., Moisture in organic coatings – a review. *Prog. Org. Coat.,* (1999) 37: 1–14.

51. Flaconneche, B., Martin, J., and Klopffer, M. H., Transport properties of gases in polymers: experimental methods. *Oil Gas Sci. Technol.,* (2001) 56: 245–259.

52. Comyn, J. *Polymer Permeability*, Elsevier Applied Science Publishers Ltd, London, 1985.

Chapter 3

Experimental procedures

3.1 Permeation test method

3.1.1 Materials

Shallow aluminium permeation cells (height 20 mm) with open top screw on lids were manufactured (see Scheme 1). Aluminium was used because it is an impermeable material and light enough to be weighed accurately on an analytical balance. An aluminium ring (inner diameter 79.70 mm, outer diameter 87.70 mm, thickness 3 mm) and nitrile butadiene rubber (NBR) gaskets (same diameters as the aluminum ring, thickness 2 mm) were used to seal the cells. NBR was supplied by Gasket & Shim Industries (Pty) Ltd. Activated carbon powder (100–400 mesh) was supplied by Sigma-Aldrich. Heptane (CP grade, 99%) was obtained from Kimix Chemicals, and is characterised by the following properties: molecular weight, M_r = 100.2019 g/mol, and saturated vapour pressure, p_s = 54.946 mbar. Mineral oil used as a component in offset printing inks was supplied by Continental Printing Inks.

Commercially available plastic films commonly used as food packaging materials were used as model packaging films. These included polyethylene terephthalate (PET), cellophane, polypropylene (PP), different polyethylene (PE) films such as high density polyethylene (HDPE), low density polyethylene (LDPE) and PE-laminated paper, as well as paperboard of different grammages (mass per unit area), and coated with barrier coatings for food contact applications. Thicknesses (µm) of the model packaging materials were measured at 23℃ and 50% r elative humidity with a micrometer.

3.1.2 Testing procedure

Desiccators were prepared to contain either an organic solvent (in this case heptane) or mineral oil. Wicks were attached to the inside walls of the desiccators, ensuring that the bottom ends hang in the solvent in order to facilitate the vapour pressure saturation point being rapidly reached. The desiccators were kept closed for at least 24 h to ensure the environment was at equilibrium. Samples of substrates were punched with a circular cutting disk. All samples had the same surface area of 6.04 x 10^{-3} m^2 (diameter = 87.70 mm), to fit perfectly between the container and the lid. About 7 g activated carbon was weighed in the container. The substrate and lid, including a three-layered seal (as shown

in Scheme 3.1) was used to close the permeation cell. After closing, the surface area of the substrate exposed to the environment was 4.99 x 10^{-3} m^2. The permeation cells were placed inside a desiccator containing the saturated environment of organic vapour, at controlled temperature of 23℃. After a designated period of time, the permeation cells were removed from the desiccator, the lid and substrate were removed, and the container was immediately weighed.

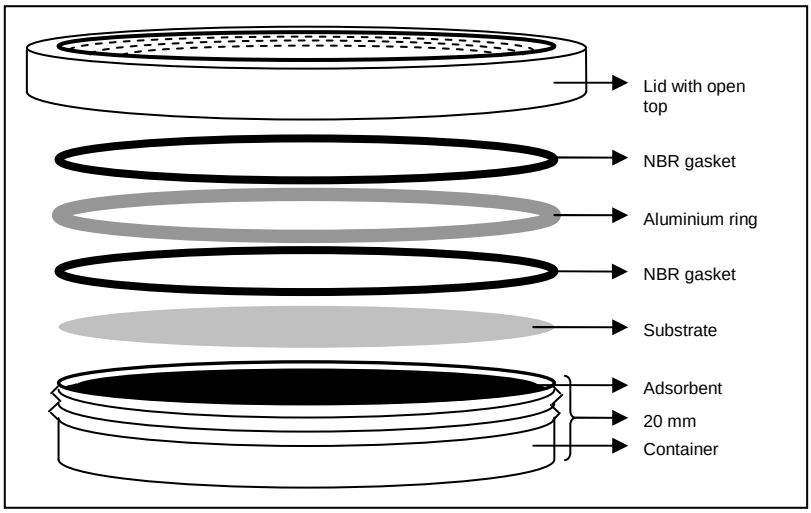

Scheme 3.1: Assembly of the permeation cell.

3.2 Organic vapour sorption

3.2.1 Materials

Penetrant, *n*-heptane (Sigma Aldrich) with a purity of 99%, were used as received. The same polymeric films as mentioned in section 3.1.1 were studied by the sorption system.

3.2.2 Instrumentation

Sorption studies of organic vapours were carried out on an Intelligent Gravimetric Analyser (IGA) from Hiden Isochema Ltd., model IGA-002. This instrument consists of a computerised microbalance with a 1 µg sensitivity. In addition, the sample temperature and gas/vapour pressure are accurately controlled, hence allowing measuring sorption isotherms, and the corresponding kinetics, of organic vapour mass uptake at various pressure steps.

3.2.3 Parameters

The samples analysed were firstly degassed under high vacuum (10^{-2} mbar) to remove any excess vapours that may be present on the surface of the sample, until a constant weight was reached. The

liquid used to generate the desired vapour (penetrant) was placed inside the vapour cell. The vapour pressure was gradually increased over a period of 1min until the desired organic vapour pressure was achieved. This period should be short compared to adsorption kinetics, but long enough so as not to disturb the microbalance. The pressure was accurately controlled by admittance and exhaust valves to maintain this pressure setting until equilibrium mass uptake was established, after which the pressure was increased to the next pressure setting. Pressure steps were in the range of p/p_0 = 0.01 to 0.9, where p is the actual vapour pressure and p_0 is the saturated pressure at that temperature. All other settings used are given in Table 3.1.

Table3.1: Parameter settings of sorption experiments

Parameter	Setting	Definition
Mode	F1	Uses the linear driving force (LDF) model for real-time analysis
Phase	0.5	Minimum setting, data acquisition starts at the midpoint of the pressure step
Minimum time	10-30 min	Minimum time to remain at a p/p_0 setpoint
Time-out	2-40 h	Maximum time to run a p/p_0 setpoint
Wait until	99%	The % of predicted absorption that must occur before continuing to the next p/p_0 setting
RTP minimum	3 µg	Minimum weight change for real-time analysis
RTP tolerance	2 µg	Acceptable average deviation from the model
Acquisition minimum	1 µg	Target interval for weight acquisition
Ramp rate	0.3-10 mbar/min	Depending on increments, but generally ~1min to reach set-point
Regulation	ON	Inlet and outlet valves remain active the entire time during each p/p_0 to maintain constant p
Temperature	23℃	Temperature at which isotherms are measured

3.2.4 Data processing

The increase in weight due to penetrant uptake by the matrix polymer as a function of time at each p/p_0 was used to calculate the kinetic parameters of adsorption, and the equilibrium mass uptake at a wide range of p/p_0 were used to create the sorption isotherms.

The diffusion coefficient, D, was calculated with the aid of IGASwin software, which uses the gradient of the linear region in the fractional mass uptake:

$\frac{M_t}{M_\infty}$ vs. $\sqrt{time}\,(s^{1/2})$ plot to solve for D, via least squares regression, in the equation:

$$\frac{M_t}{M_\infty} = 1 - \sum_{n=0}^{\infty} \frac{8}{(2n+1)^2 \pi^2} \exp\left[\frac{-D(2n+1)^2 \pi^2 t}{l^2}\right] \qquad \textbf{Eq. 3.1}$$

The solubility coefficient was calculated as the ratio between the equilibrium penetrant concentration in the film, c, and the organic vapour pressure, p:

$$S = \frac{c}{p} \qquad \textbf{Eq. 3.2}$$

The equilibrium penetrant concentration was calculated from:

$$c = \frac{M_\infty - M_0}{V_p M_{VOC}} \times V_m \qquad \textbf{Eq. 3.3}$$

where M_0 and M_∞ are the initial and equilibrium mass of the polymer matrix (in mg), V_p is the volume of the polymer (in cm^3), M_{VOC} is the molecular weight of the penetrant (in g/mol) and V_m is the molar volume of the penetrant at standard temperature and pressure (STP) (in cm^3/mol).

The permeability coefficient, P, was determined from the solution-diffusion model which states that the permeability is equal to product of the diffusion and solubility coefficients:

$$P = D \times S \qquad \textbf{Eq. 3.4}$$

Chapter 4

Permeation test method

4.1 Introduction

Overview of available test methods for evaluation of oil penetration in paperboard:

The technical association of the pulp and paper industry (TAPPI) creates standard test methods for evaluation of pulp and paper products. There is currently no test method for measuring mineral oil migration from paperboard into food. However, several TAPPI standard methods and TAPPI useful methods (UMs) are available to evaluate paper and board properties in terms of grease or oil resistance characteristics, i.e. resistance to penetration of oil in its condensed form from the food into the paper. The most familiar test method used in the paper industry is the grease resistance test for paper and paperboard, T559 or UM557, also known as the “kit test” [1]. This kit test involves 12 different solutions each containing different ratios of castor oil, toluene, and *n*-heptane. The ability of each kit solution to penetrate into paper is more pronounced from number 1 through to 12. A drop of the highest kit solution is placed on the paperboard surface for 15s, after which it is wiped off and the surface inspected for damage. This process is repeated with lower numbered kit solutions, and the highest number solution that does not leave a mark on the surface, indicates what is known as the kit rating of the product. This method is quite popular, as it can be utilised for paperboard coated with a grease barrier coating, and is thus a “one-sided” method. Commercially available grease or oil barrier coatings are usually classified according to their kit ratings.

Other test methods for grease or oil resistance are available, but these do not necessarily apply to coated paperboard with the functional barrier on only one side, as these tests consider both sides of the packaging. The UM407: Oil absorption of paperboard test method is usually used for paper intended to pack bakery food products [2]. This method evaluates the resistance of paperboard to penetration of vegetable oil. A standard size paperboard sample is dipped into warm vegetable oil at 71℃ for 30s, after which it is wiped dry. The grea se absorption is reported as the percentage increase in weight. Similarly, the absorbency of paperboard towards heavy mineral oil is measured according to UM418, but here the mineral oil is kept at room temperature. This method is used to correlate the amount of oil absorption to the wax required in wax-paper applications.

Oil penetration of paper and paperboard (UM410) is also evaluated by measuring the amount of time it takes for a coloured/dyed oil to penetrate the test sample and subsequently become visible on the opposite side. T462 describes the permeation of castor oil through paper by measuring the time required for a drop of castor oil to progress through the paper and finally make a translucent drop on the under side of the test sample [3]. T454 turpentine test for grease resistance of paper [4] also measures the time for coloured turpentine to penetrate from one side of a test sample to the other side, whereas T507 grease resistance of flexible packaging materials [5] determines the average stained area when either vegetable or mineral oil penetrated through a test sample and stained blotting paper on the other side. Similar to these mentioned TAPPI methods, the oil or grease penetration rate of flexible barrier materials can also be determined according to ASTM F-119 [6]. In this method, the barrier film is placed between an oil- or grease-soaked cotton disk, and a ground glass backing plate. The time required for the first indication of wetting of the glass backing plate indicates the rate of grease penetration. However, it has been reported that this method is quite primitive and that significantly high standard deviations were obtained [7].

This chapter reports on a new test method that can be used to quantitatively evaluate the migration of organic contaminants present in paper and plastic packaging into foodstuffs via the vapour phase.

4.2 Principle of the proposed new test method

Diffusion of volatile organic compounds (VOCs) through substrates can be measured by two different methods: sorption or permeation. The method reported in this work uses a permeation cell similar to that used in a TAPPI test method for determination of the moisture vapour transmission rate of paper and paperboard [1]. This test cell works on the concept of permeation as depicted in Scheme 4.1. The inside of the cell is filled with an adsorbent material, and the substrate is sealed onto the open mouth of the cell, with known area. The cell is then placed in a controlled environment of organic vapour pressure and temperature conditions. It is assumed that the penetrant (organic vapour) is thus present at constant high partial pressure, p_1, on the one side of the substrate and constant low pressure, p_2, on the other side of the substrate, on the inside of the cell. This causes a constant pressure differential ($p_1 >> p_2$), which is the driving force for organic vapour flux through the substrate. Diffusion of the penetrant through the substrate, and subsequent adsorption onto the adsorbent, allows gravimetric

monitoring of the amount of organic vapour that permeates through the substrate by weighing the adsorbent periodically. Keeping the cell in a constant environment of temperature and penetrant partial pressure (i.e. when p_1 and p_2 on both sides of the substrate are constant) leads to a constant diffusion rate of the penetrant through the substrate (and thus linear weight uptake as a function of time). This is known as the steady-state permeation [8]. The quantity of organic vapour that passes through a unit area of the substrate may be plotted as a function of time in order to obtain the permeation curve. The slope of this curve under steady state conditions gives the transmission rate of the organic vapour through the substrate.

For example, when heptane is used as the organic vapour, the heptane vapour transmission rate (HVTR) can be defined as the mass of heptane-saturated vapour transmitted per unit of surface area of a specific substrate per hour, and can be calculated by the following equation:

$$\frac{wt_2 - wt_1}{A \cdot t} = HVTR\,(g / m^2 / h) \qquad \textbf{Eq. 4.1}$$

where wt_1 and wt_2 are the weights of activated carbon before and after exposure, respectively (measured in grams), A is the area of the exposed substrate (measured in square meters), and t is the time (measured in hours).

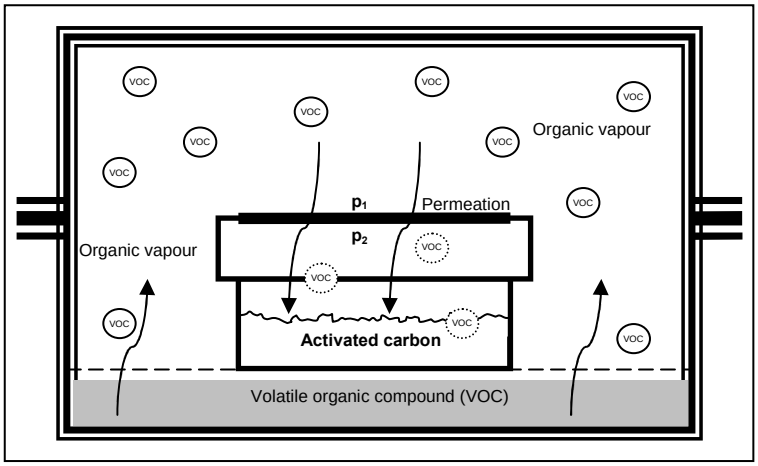

Scheme 4.1: Permeation set-up.

The penetrant could be any organic hydrocarbon that resembles mineral oils, but generally a lower molecular weight compound, such as heptane (C_7H_{16}) or octane (C_8H_{18}), would facilitate even higher diffusion rates as already achieved by the concentrated environment, thus allowing a highly accelerated method. Activated carbon is a type of carbon with a very high specific surface area [9]. Its

highly porous structure allows for the adsorption of impurities. It is often used in gas purification filters to remove oil vapour and other volatile organic hydrocarbons. Activated charcoal is therefore considered as a suitable adsorbent of organic vapour or mineral oil in this new test method. Its porous structure also resembles dry foods with high surface area, which are most commonly packed in paperboard packaging and which are reported as quite susceptible to the migration of organic hydrocarbons [10-12].

4.3 Results and discussion

4.3.1 Evaluation of heptane and activated carbon as suitable simulants

Heptane was selected as a possible simulant for mineral oil (MO), and activated carbon as a simulant for dry foodstuff. An open test cell containing only activated carbon and no substrate was placed inside the saturated organic vapour environment. Figure 4.1 (a) shows the adsorptive capacity of activated carbon to adsorb MO vapour. The MO vapour was adsorbed readily by the activated carbon, and full adsorption capacity was not reached even up to 13 days exposure time. Figure 4.1 (b) shows the adsorptive capacity of activated carbon towards heptane vapour at 23℃ under a saturated atmosphere of heptane. The activated carbon was able to adsorb heptane vapour up to more than 50% of its weight. Rapid adsorption occurred in the first hour of exposure, after which the rate of adsorption started decreasing and finally the activated carbon became saturated with heptane after about 4 h exposure time in an open cell. This indicates that heptane as a MO simulant will be adsorbed much more rapidly than actual MO vapour, due to the smaller size of the heptane molecules, and a higher partial vapour pressure at room temperature. Heptane and activated carbon were thus the selected candidates for MO simulant and dry food simulant, respectively.

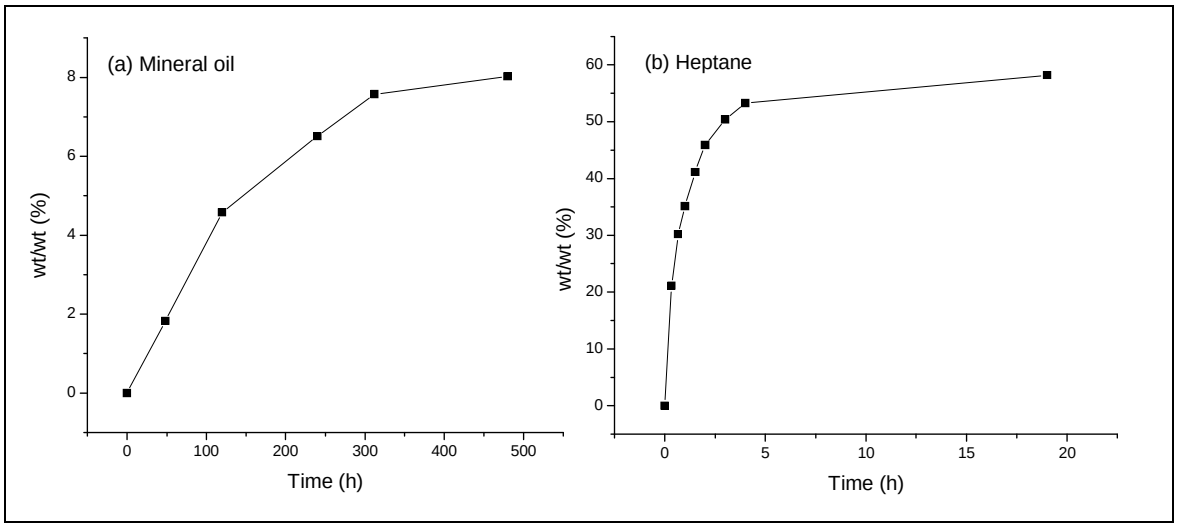

Figure 4.1: Adsorptive capacity of activated carbon for (a) mineral oil and (b) heptane vapour.

4.3.2 Evaluation of the sealing efficiency

One of the most important aspects of the efficiency of the method is to establish an efficient sealing between the substrate and the permeation cell in order to ensure the weight uptake measured is only due to the permeation of heptane through the substrate. A standard barrier benchmark material such as aluminium foil, impermeable to organic vapours or MOs as such, was utilised to evaluate the efficiency of the sealing system. A permeation cell with this benchmark material as the substrate (aluminium foil with a thickness of 100 µm) in the lid was placed inside the prepared desiccator. Different sealing materials were evaluated as the seal, namely Teflon®, cork, polyvinylchloride (PVC), and NBR. The adsorbent showed no detectable weight gain (with an uncertainty associated with the method of ± 0.10 g/m^2/h) when NBR was used as the sealing material. This served to confirm that no organic vapour passed through the impermeable benchmark substrate, and also not through the connection points in the seal. NBR is characterised by good swelling resistance in mineral oils, and allows for some compression when closing the lid, which prevents damage of the substrate surface. NBR, therefore, yielded a suitable sealing where the other materials evaluated failed.

4.3.3 Evaluation of model packaging materials

The transmission of MO vapour through various typical food packaging materials is shown in Figure 4.2. These materials included polymeric films, plastic laminated paper, uncoated paperboard (PB), and PB coated with a coating configuration likely to give good barrier properties to MO vapour. The MO mass uptake per unit area shows a constant increase for the polymer films and coated PB, as a function of time, measured over a 10 day period. For uncoated PB samples, a deviation from

linearity in the mineral oil vapour transmission rate (MOVTR) was reached within 10 days. This is most likely the result of highly permeable materials allowing high quantities of MO vapour to permeate through the substrate, and subsequently the vapour pressure on the inside of the permeation cell, p_2, increases. Even though the activated carbon has not reached its full adsorptive capacity, the fast transmission rate and subsequent change in pressure through highly permeable materials lead to a decrease in the apparent transmission rate after about 5 days. It is therefore recommended that the actual transmission rate be measured from the steady state conditions (all calculated transmission rates are reported in Table 4.1). Furthermore, PB is a porous material, and therefore not considered as a barrier material towards volatile compounds [13]. Uncoated PB samples, produced from the same constituents, and differing simply in grammage (mass per unit area), exhibited higher transmission rates when the board grammages decreased. The MOVTR increased from 4.75 to 6.52 g/m^2/day as the grammage was reduced from 400 to 250 g/m^2. It is evident that boards with higher porosity will exhibit faster organic vapour migration rates compared to less porous boards with higher grammages. The same effect was found with the migration of phthalates from PB into Tenax [14].

The MOVTR through uncoated PB was also found to be much higher than the polymeric materials, such as polyethylenes, considered to be poor MO barriers, e.g. high density polyethylene (HDPE) and a PE-laminate. PB will allow easy migration of organic vapours into foodstuff if no barrier is utilised, but coated board may act as a barrier to organic vapours, as was found with the coated PB 300 g/m^2 sample. The MOVTR of 300 g/m^2 PB was reduced from 4.14 g/m^2/day for the uncoated sample to 0.9 g/m^2/day for the coated sample. Results also confirmed that polyethylene terephthalate (PET) and polypropylene (PP) are very good barriers to MO vapour, as reported elsewhere [15].

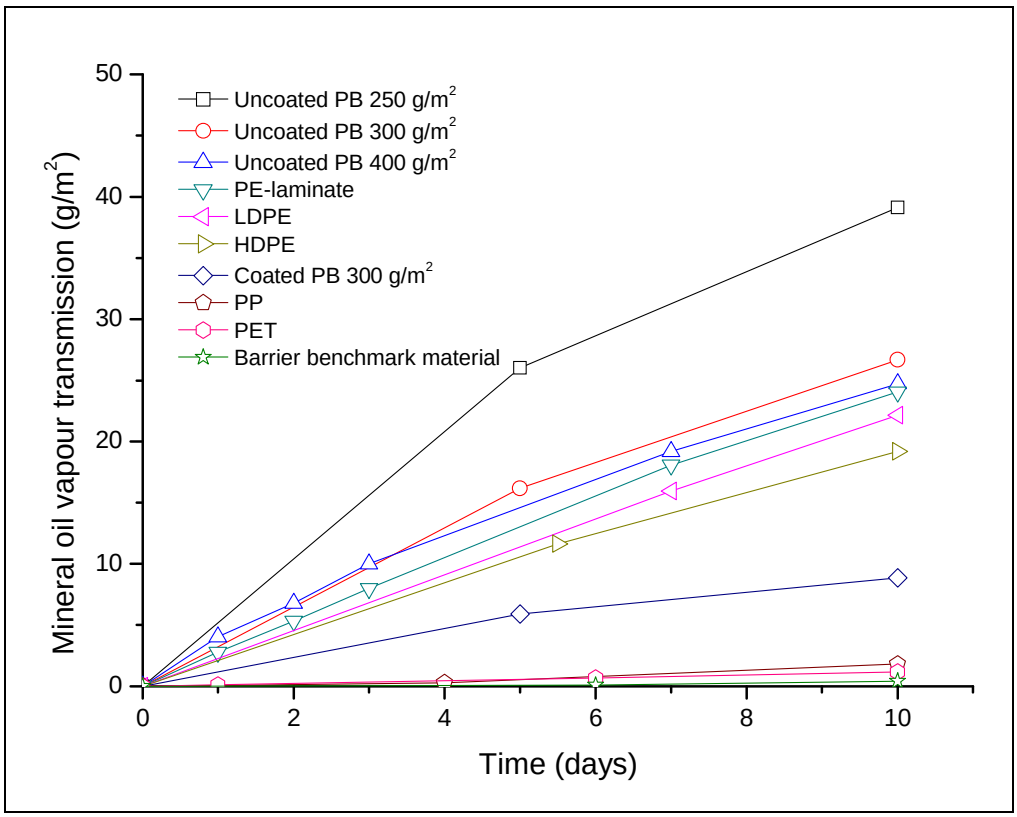

Figure 4.2: Mineral oil vapour transmission through various food packaging materials over a period of 10 days.

Heptane was utilised as the penetrant in the accelerated test method, and HVTRs were measured over a period of 8 h. Figure 4.3 shows that PET and PP exhibit excellent heptane vapour barrier properties (similar results were found for MOVTR). A similar trend as observed for the uncoated paperboard with the lowest grammages was observed, namely, the HVTRs started to decrease after 1–2 h. However, for packaging materials with somewhat better organic vapour barrier properties, the HVTR was found to be constant over a period of 8 h, showing a steady state of organic vapour permeation.

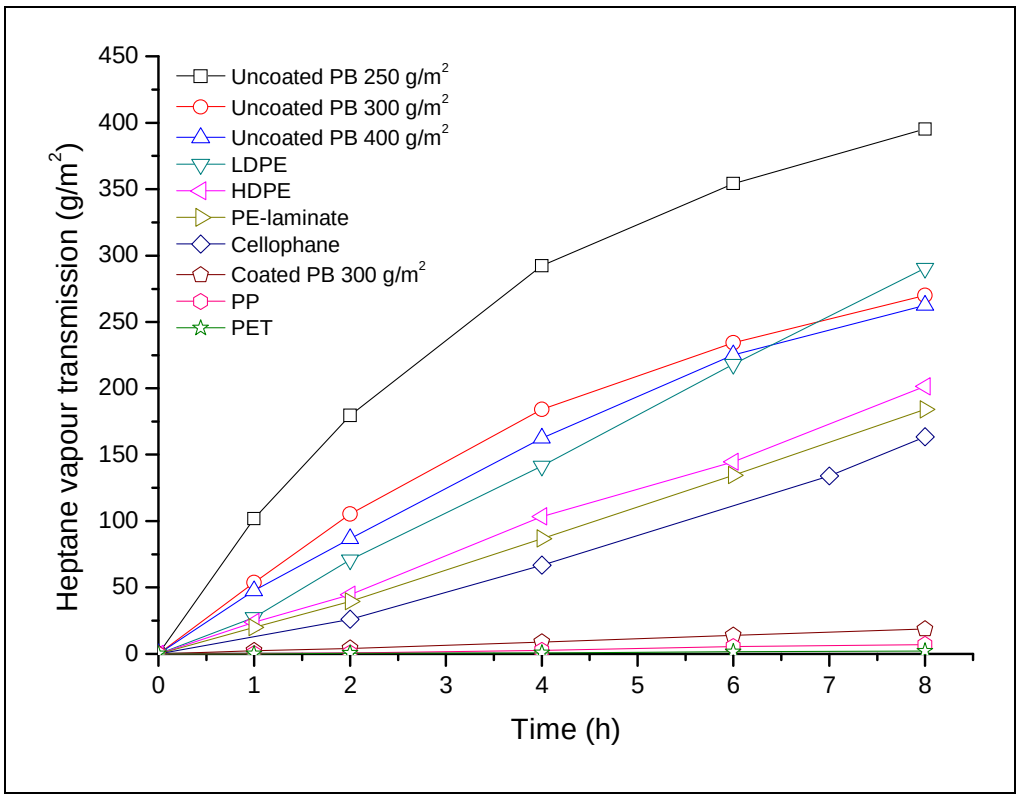

Figure 4.3: Heptane vapour transmission through various food packaging materials over a period of 8 hours.

Table 4.1: MOVTR and HVTR values of different food packaging substrates

Substrate	**MOVTR (g/m^2/day)**	**HVTR calculated from steady state conditions (g/m^2/h)**	**HVTR experimentally determined within 1 h (g/m^2/h)**
Barrier benchmark material	0.00	0.10	0.00
PET	0.23	0.24	0.11
PP	0.25	0.55	0.25
LDPE	2.20	35.43	30.75
HDPE	1.84	25.08	26.12
PE-laminate	2.52	23.13	22.68
Uncoated PB 400 g/m^2	3.37	40.14*	47.76
Uncoated PB 300 g/m^2	4.14	45.65*	59.10
Uncoated PB 250 g/m^2	5.45	71.52*	105.09
Coated PB 300 g/m^2	0.90	2.36	3.04

*Steady state conditions for uncoated PB samples were achieved within 4 h, whereas for all other samples it was calculated within 8 h.

In order to establish whether HVTR values are representative of true MOVTR, MOVTR values were plotted against HVTR values (calculated from steady state conditions), as shown in Figure 4.4. A linear correlation between MOVTR and HVTR values, with a correlation factor of 0.987, indicates that heptane constitutes a good simulant for MOs, and can be accordingly used as a means of evaluating the ability of barrier protective coatings to prevent the migration of MO from packaging into foodstuff.

Results in Figure 4.3 showed that even a measuring time as low as 1 h was sufficient to distinguish between the heptane vapour transmissions through different materials. HVTR values calculated over a period of up to 8 h, depending on the steady state conditions, proved to be well correlated to the HVTR values determined over 1 h, as shown in Figure 4.5. For poor barriers, such as uncoated PB, the HVTR measured at 1 h was higher due to the initial fast transmission of heptane through these porous substrates. Most of the other packaging substrates evaluated showed a slightly lower HVTR measured in 1 h. In addition, a relatively high deviation was observed for very good barrier materials such as PP and PET, as the calculated HVTR after 8 h (0.55 and 0.24 g/m^2/h, respectively) was found to be about 2 times higher than the HVTR experimentally determined after 1 h (0.25 and 0.11 g/m^2/h, respectively). This may be a result of a longer time lag taking place at the onset of permeation, which is found in polymer films with low permeability when the concentration of the penetrant varies throughout the film as a function of time [8]. In these cases, steady state diffusion conditions only occur once a constant penetrant concentration is reached throughout the film thickness. This effect was more evident for very good barrier materials, and in such cases it may be necessary to increase the measuring time in order to ensure the calculated HVTR values are representative of the actual permeation of the barrier material.

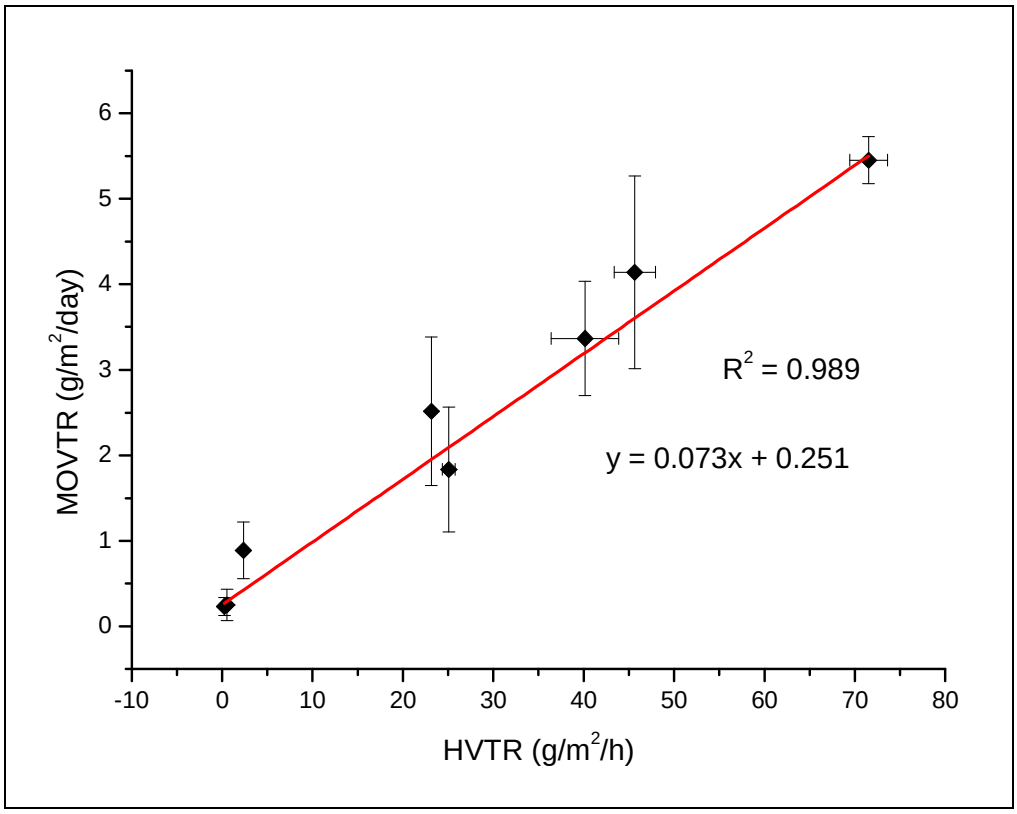

Figure 4.4: Correlation between mineral oil and heptane vapour transmission rates.

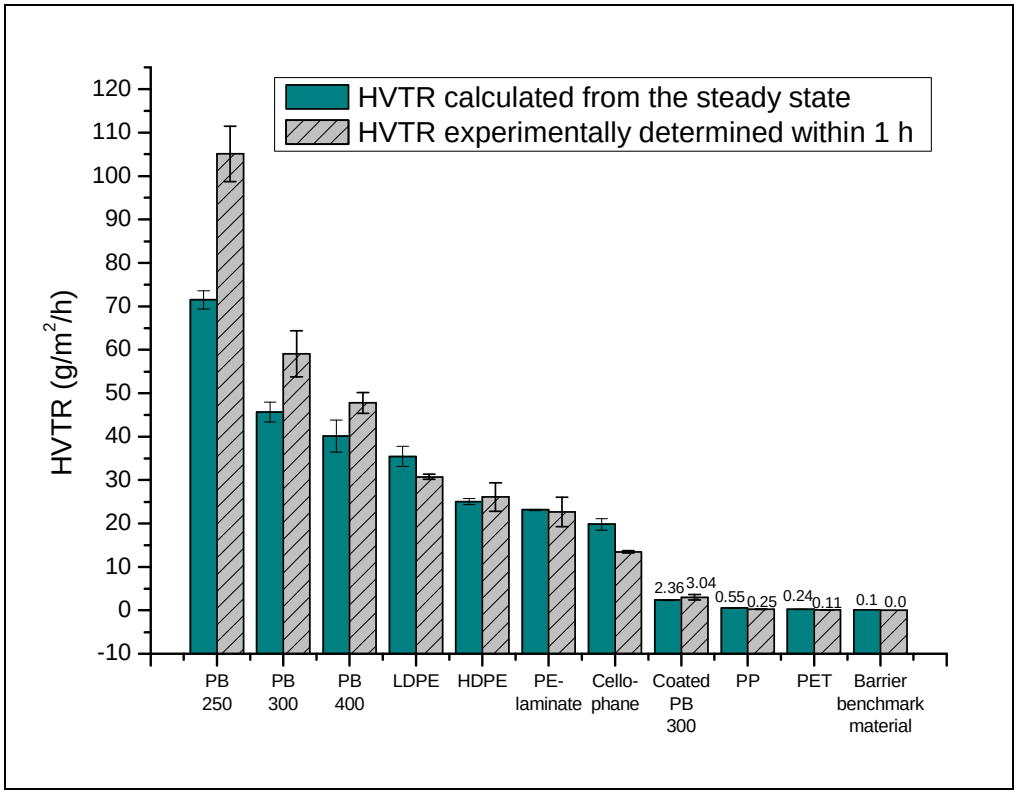

Figure 4.5: HVTR calculated from steady state conditions and experimentally determined within 1 h of paperboard and polymeric films.

4.4 Transport parameters derived from HVTR

The abovementioned test method is rather rich in information, and can be used to derive the most important transport parameters which are required to interpret MO migration. The next section focuses on deriving these parameters, especially those needed to interpret the behaviour of materials containing MO in real conditions of food packaging applications. These derivations are illustrated in Scheme 4.2, and the assumptions made throughout are numbered a) – e). Since a good agreement was found between HVTR and MOVTR (section 4.3.3 above), the permeability coefficient (section 4.4.1) and flux, as obtained with the short HVTR method, was used to derive the flux of MO in real conditions of use (section 4.4.2). From there, the diffusion coefficient of MO in the model packaging materials could be calculated (section 4.4.3), which could finally be used to interpret actual MO migration through plastic and paper packaging into dry foodstuffs (section 4.5), and the subsequent product shelf-life (section 4.6).

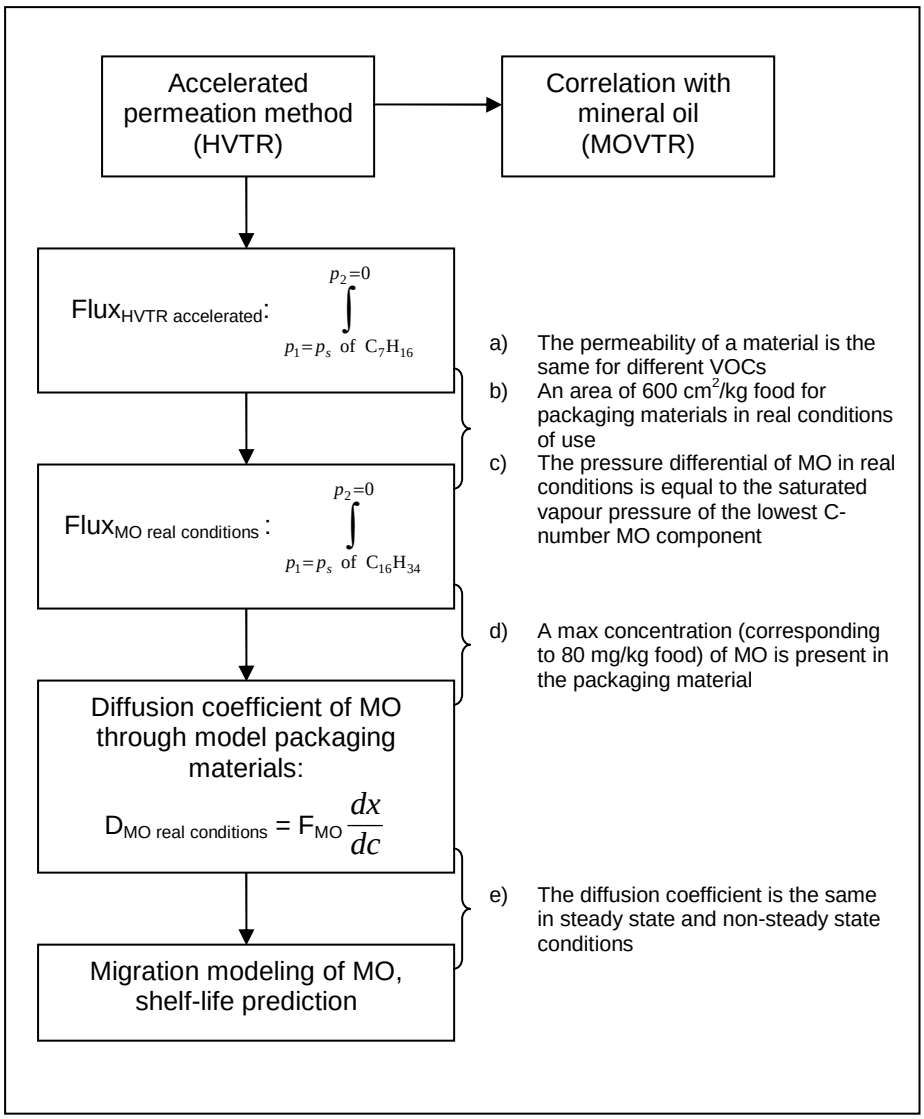

Scheme 4.2: Derivations and assumptions to interpret results from the short HVTR method in terms of real life MO migration from packaging materials into food.

4.4.1 Permeability and diffusion coefficients

Determination of the permeability coefficient, P, includes the effect of material thickness according to:

$$P = \frac{transmission\ rate \times l}{\Delta p} \qquad \textbf{Eq. 4.2}$$

where l is the thickness of the substrate, and Δp is the partial pressure difference between the two surfaces. Permeability is a measure of how easily the penetrant is transported through the material. The permeability coefficient is defined as the volume of penetrant that flows through a unit area of material in unit time, where a unit pressure difference is maintained. Therefore, P is calculated from permeation data by:

$$P = \frac{Ql}{A(p_1 - p_2)t} \qquad \textbf{Eq. 4.3}$$

where Q (cm^3) is the vapour volume in relation to the molar volume of a gas at standard temperature and pressure (STP, 0℃, 101.325 kPa) that permeated in the time interval, t (s), A is the substrate area (cm^2), l is the film thickness (cm), and p_1 and p_2 are the upstream and downstream pressures (mbar), respectively. Then P is expressed in standard units of cm^3(STP)cm/cm^2.s.mbar. Since $p_2 << p_1$, p_2 was assumed to be zero [16]. An example of the average plot of $\frac{Ql}{A(p_1 - p_2)}$ vs. t for PP is shown in Figure 4.6 where the slope is equal to P. Calculated permeability coefficients are given in Table 4.2. Of the polymeric films tested, PET showed the lowest permeability towards heptane vapour, and PP exhibited only slightly higher permeability, similar as to the trend observed in HVTR of these two materials. Despite a significant difference found in their permeability coefficients, HDPE, LDPE, and PE-laminate exhibited similar HVTR properties. This could be explained by the effect of the film thickness. For example, the PE-laminate evaluated was 10 times thicker than the HDPE film, with a permeability coefficient 10 times greater. HVTR does not take the thickness of a material into account and therefore it appears as though these materials perform the same towards heptane vapour. However, the permeability coefficient illustrates that, when they all have the same thickness, HDPE would perform as a better barrier to heptane vapour transmission, as compared to LDPE and PE-laminate. Similar to the findings with HVTR, the permeability of PB substrates are up to 3 orders of magnitude higher than that of polymer films. Calculation of P of coated PB becomes more complex, as this could be considered a multilayer substrate [17]. For simplicity, P was calculated for the polymer coating only. The permeability was reduced to the same range as that of good MO barriers, PET and PP. This was also reflected in the MOVTR and HVTR results where the coated PB sample showed a transmission rate just higher than that of PET and PP.

Furthermore, the diffusion coefficients were determined by means of the time lag method. This follows from the initial conditions when the penetrant is firstly introduced at the one side of the polymer film in the permeation cell, and a constant penetrant concentration throughout the thickness of the film has not yet been established [8]. Once the steady state conditions have been reached, the x-intercept of the permeation curve is used to determine the diffusion coefficient according to:

$$D = \frac{l^2}{6\theta} \qquad \textbf{Eq. 4.4}$$

where θ resembles the x-intercept in Figure 4.6. Values for D are given in Table 4.2, and were mostly in the same order of magnitude for the materials tested, except for LDPE which had the highest diffusion coefficient. Due to the extremely fast heptane vapour transmission through uncoated PB, a time lag period could not be identified for these materials, and therefore no diffusion coefficient was calculated.

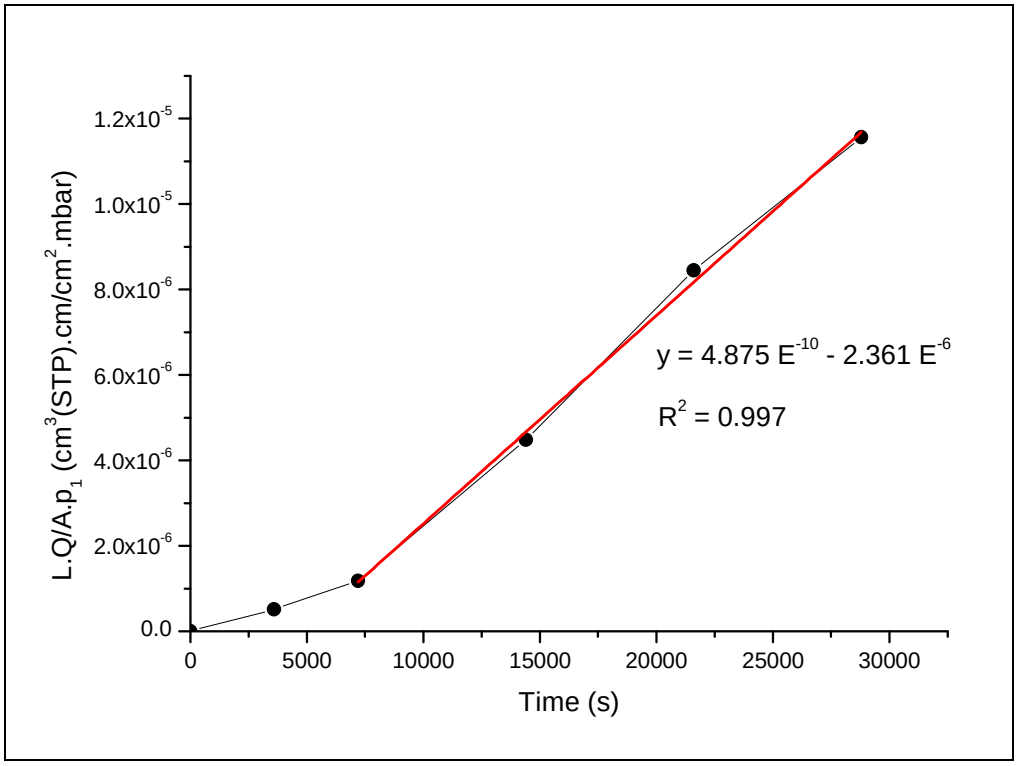

Figure 4.6: Average permeation curve of PP showing the time lag.

Table 4.2: Permeability and diffusion coefficients from permeation experiments

Substrate	l (cm)	P (cm^3(STP)cm/cm^2.s.mbar)	D (cm^2/s)
PET	0.011	4.64 E^{-10}	5.35 E^{-10}
PP	0.005	4.88 E^{-10}	2.15 E^{-10}
Cellophane	0.0025	6.20 E^{-9}	3.65 E^{-10}
HDPE	0.001	3.02 E^{-9}	7.10 E^{-10}
LDPE	0.005	1.65 E^{-8}	1.33 E^{-9}
PE-laminate	0.010	2.69 E^{-8}	9.86 E^{-10}
PB 250 g/m^2	0.032	2.58 E^{-7}	#
PB 300 g/m^2	0.039	1.97 E^{-7}	#
PB 400 g/m^2	0.054	2.09 E^{-7}	#
Coated PB 300 g/m^2	0.0024	6.55 E^{-10}	5.14 E^{-10}

D of uncoated PB could not be determined by the time-lag method, since permeation rates were too fast

4.4.2 Flux of mineral oil

The methods described by MOVTR and HVTR are essentially a measure of the flow of organic vapour (also known as the flux) through a packaging material. Given a constant concentration of organic vapour on both sides of the film in the permeation cell, the steady state conditions are described by Fick's first law that states that the diffusive flow, F, is proportional to the concentration gradient throughout the thickness of the film, $\frac{dc}{dx}$, and is given by:

$$F = -D\frac{dc}{dx} \qquad \textbf{Eq. 4.5}$$

The negative sign indicates that the flow occurs from a high concentration side, c_1, to a low concentration side, c_2. In cases where the surface concentrations c_1 and c_2 are not known, the vapour pressures on either side of the film, p_1 and p_2, may be used to describe the flow, given as:

$$F = -P\frac{dp}{dx} \qquad \textbf{Eq. 4.6}$$

where P is the permeability coefficient [8]. This relationship is illustrated by Scheme 4.3 of the steady state conditions. The boundary conditions supposed in this state includes a constant infinite concentration/pressure at the high activity side, and a zero concentration/pressure at the low activity

side. In addition, the film is initially at zero concentration of the migrant, $c_0 = 0$, and is notable from the characteristic time-lag observed in permeation experiments.

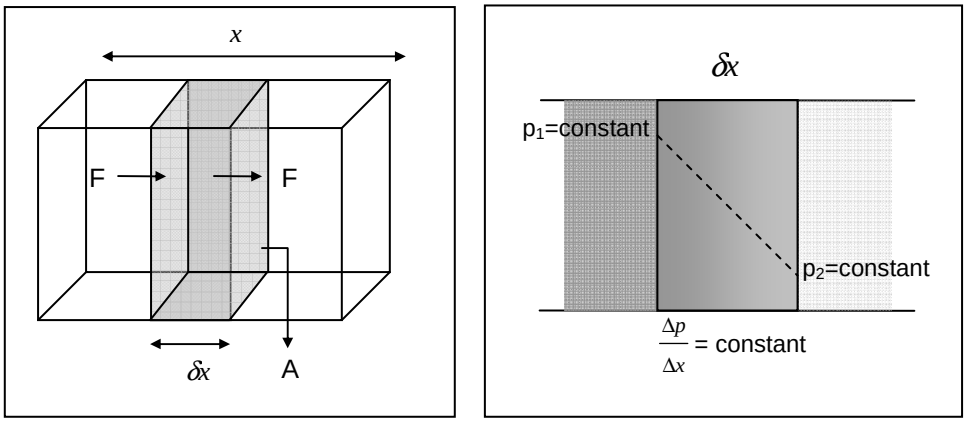

Scheme 4.3: Steady state conditions of constant flow.

The flow of heptane vapour (in cm^3/s) through the different model packaging materials was determined from equation 4.6, and therefore:

$$\int_{x=0}^{x=l} F dx = -\int_{p_1=54.9}^{p_2=0} P dp \qquad \textbf{Eq. 4.7}$$

The saturated vapour pressure of heptane at 23℃ is 54.9 mbar, and assuming a heptane partial pressure inside the permeation cell equal to zero, the flow of heptane can be determined through each of the tested packaging materials across the thickness of the film for the entire exposed area. From equation 4.7 it can be written that:

$$F = P\left[\frac{cm^2}{s.mbar}\right] \times \frac{54.9-0}{l}\left[\frac{mbar}{cm}\right] \qquad \textbf{Eq. 4.8}$$

Then the total flow becomes:

$$F\,(total) = P\left[\frac{cm^2}{s.mbar}\right] \times \frac{54.9-0}{l}\left[\frac{mbar}{cm}\right] \times A\left[cm^2\right] \qquad \textbf{Eq. 4.9}$$

Values of F are given in Table 4.3. In order to predict the transport behaviour of MO based on the findings from HVTR, it would have to be assumed that the permeability of the films towards heptane vapour is the same for the higher molecular weight MO commonly found in packaging materials. Then the flow of MO could simply be determined by considering the saturated vapour pressure of MO in

equation 4.7. This was derived from the component in a MO mixture (a range of materials from C_{16}–C_{24}) with the highest vapour pressure, namely hexadecane ($C_{16}H_{34}$), in order to give the smallest pressure differential and therefore the fastest flow (worst case) achievable. The saturated vapour pressure of *n*-hexadecane is 0.0019 mbar at 23℃ [18]. Therefore, the flow of MO in the model packaging materials can be described in the same way as for heptane:

$$\int_{x=0}^{x=l} F dx = -\int_{p_1=0.0019}^{p_2=0} P dp \qquad \textbf{Eq. 4.10}$$

Results of F_{MO} in real conditions of use are given in Table 4.3.

4.4.3 Transport parameters that resemble real conditions of use

Since it is possible to describe the flow of MO through the tested materials, from equation 4.5 it is also possible to determine the diffusion coefficients of MO in the model packaging materials. This means that if it is assumed that the diffusion coefficient of MO in packaging materials remains constant, regardless of the concentration, the diffusion of MO in real conditions of use could also be explained. From equation 4.5, the diffusion coefficient of MO in the model packaging materials were determined using the flow (in mole/cm^2.s^{-1}) as determined in 4.4.2, and the concentration of MO (in moles/cm^3) was determined from a concentration that corresponded to 80 mg/kg food. Previous research on the MO content in packaging materials showed that the highest concentration was found in recycled PB and corresponded to 80 mg/kg food [15]. The diffusion coefficients are given in Table 4.3. Uncoated PB samples, followed by PE-laminate and LDPE were found to exhibit the highest diffusion coefficients. Cellophane was found to have an intermediate diffusion coefficient, followed by PET and HDPE. PP and the barrier coated PB demonstrated the lowest diffusion coefficients.

Table 4.3: F of HVTR under accelerated conditions, and derived values of F and D for MO in real conditions of use

Material	F of heptane (HVTR) (cm^3/s)	F of MO in real conditions of use (cm^3/s)	D of MO in real conditions of use (cm^2/s)
PET	1.16×10^{-4}	4.81×10^{-8}	7.33×10^{-13}
PP	2.68×10^{-4}	1.11×10^{-7}	3.51×10^{-13}
Coated PB 300 g/m^2	7.49×10^{-4}	3.11×10^{-7}	2.26×10^{-13}
Cellophane	6.81×10^{-3}	2.83×10^{-6}	2.23×10^{-12}
PE-laminate	7.38×10^{-3}	3.07×10^{-6}	3.87×10^{-11}
HDPE	8.29×10^{-3}	3.44×10^{-6}	4.34×10^{-13}
LDPE	9.06×10^{-3}	3.76×10^{-6}	1.19×10^{-11}
PB 400 g/m^2	1.06×10^{-2}	4.41×10^{-6}	1.62×10^{-9}
PB 300 g/m^2	1.39×10^{-2}	5.76×10^{-6}	1.10×10^{-9}
PB 250 g/m^2	2.21×10^{-2}	9.19×10^{-6}	1.19×10^{-9}

4.5 Mineral oil migration in real conditions of use

As previously mentioned, real conditions of use of contaminated packaging materials does not reflect the steady state conditions, and could be best described by Fick's second law, which is given by:

$$\frac{dc}{dt} = D\frac{d^2c}{dx^2} \qquad \textbf{Eq. 4.11}$$

The concentration of the contaminant in the film changes over time, as does the pressure gradient across the film. This is illustrated in Scheme 4.4, which shows that the flow and the pressure gradient is a function of time. The solution to Fick's law depends on the boundary conditions, which are now considered as a finite volume of penetrant that diffuses through a film into a finite volume, for resembling real conditions of use. This means that a limited amount of the contaminant is supplied on the one side, and the concentration falls as it enters the food/simulant on the other side of the film.

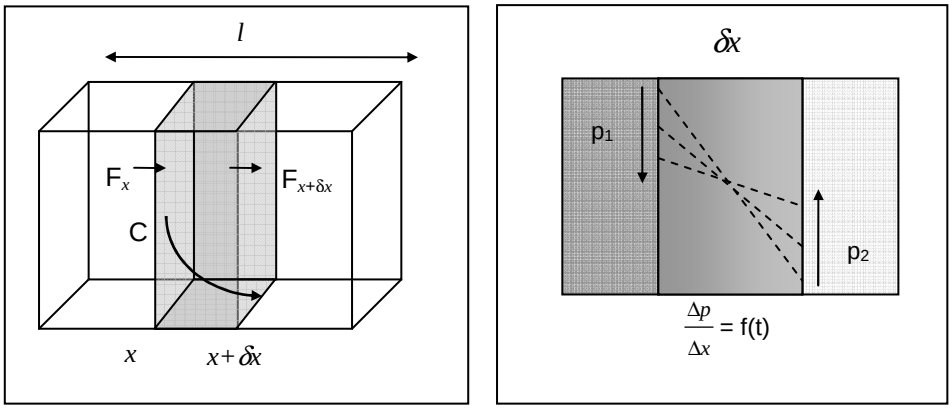

Scheme 4.4: Non-steady state conditions.

Fick's equation was previously resolved for diffusion in a plane sheet, with the abovementioned boundary conditions [19], and is given by:

$$\frac{M_t}{M_\infty} = 1 - \sum_{n=1}^{\infty} \frac{2\alpha(1+\alpha)}{1+\alpha+\alpha^2 q_n^2} \exp\left[\frac{-Dq_n^2 t}{l^2}\right] \qquad \textbf{Eq. 4.12}$$

with $\alpha = \frac{1}{K_{P/F}} \frac{V_F}{V_P}$ **Eq. 4.13**

and $\tan q_n = -\alpha q_n$ **Eq. 4.14**

where M_t is the mass transfer to foodstuff at time, t, M_∞ is the corresponding mass at infinite time (equilibrium), D is the diffusion coefficient, l is the thickness of the film, V_P is the volume of the polymer (cm^3), V_F is the volume of the food (cm^3), and $K_{P/F}$ is the partition coefficient of the migrant between polymer and food. This equation was further refined by Piringer et al. in order to introduce the initial concentration of migrant in the sheet, and obtained [20]:

$$\frac{M_{F,t}}{A} = c_{P,0}\rho_P l\left(\frac{\alpha}{1+\alpha}\right) \times \left[1 - \sum_{n=1}^{\infty} \frac{2\alpha(1+\alpha)}{1+\alpha+\alpha^2 q_n^2} \exp\left(-Dt\frac{q_n^2}{l}\right)\right] \qquad \textbf{Eq. 4.15}$$

where $c_{P,0}$ is the contaminant concentration in the film at t = 0, and ρ_P is the density of the film. This equation, describing the migration of contaminants per unit area of packaging into foodstuff, has been used extensively to model the migration of many contaminants and subsequently predict product shelf-life [21-25]. It was derived from assumptions that lead to migration predictions with sufficient margins of overestimation. The food contact material, P, is considered as a homogeneous monolayer polymeric film with a constant thickness, which is in contact with food, F, of a constant volume and surface area. In addition, it is assumed that the migrant is distributed homogeneously in P, and that no resistance to mass transport in F exists. Interactions between P and F are negligible and no swelling

of P by uptake of F occurs during migration, which results in a constant diffusion coefficient of migrant in P that doesn't change over time. Lastly, it is assumed that the concentration of the migrant in P and F remains constant during the migration process, thus not taking into consideration any occurrences such as chemical decomposition or evaporation of the migrant.

The following parameters were used in the migration modeling:

D: derived according to equation 4.5 and given in Table 4.3

$C_{P,0}$: corresponding to the highest concentration (80 mg/kg food) of MO that could potentially migrate from recycled paper packaging into dry foodstuff [15]

ρ_P : highest density of the polymer, g/cm^3

l : thickness of the polymer, cm

Area to volume ratio of packaging and food = 6 dm^2/kg food [26]

V_F = max volume of 1kg food, 1000 cm^3

V_P = max area (600 cm^2), multiplied by the thickness (cm), of the polymer, cm^3

$K_{P/F}$ = 1 for worst case assumptions

q_n values for $\alpha = \infty$ as given by Crank were used [19]

The migration of MO into foodstuff through different packaging materials was calculated at different time intervals using equation 4.15 and the parameters described above, and the resulting migration behaviour for each material is illustrated in Figure 4.7. The trends in migration coincide well with the HVTR results, in which the order of VOC transport ability through the materials is: uncoated PB > polyethylenes > cellophane > barrier coated PB > PP > PET. These findings also correlate well with previous research by Grob and co-workers that showed that PET and PP packaging materials generally have longer shelf-lives before a certain migration limit is reached, as compared to PB and PE films [15]. They analysed the MO content in food originating from PB as secondary packaging, with various types of polymer films as primary packaging. They expressed the amount of MO that diffused through the primary packaging as a percentage of the migration potential in order to get an idea of the barrier properties obtained with each type of film. They found that, after a few months of storage but not yet reaching the specified product shelf-life, PET allowed an average migration of 1%, PP of 2%,

and PE of 33%, which correspond to the barrier properties as found for these materials with the new HVTR method.

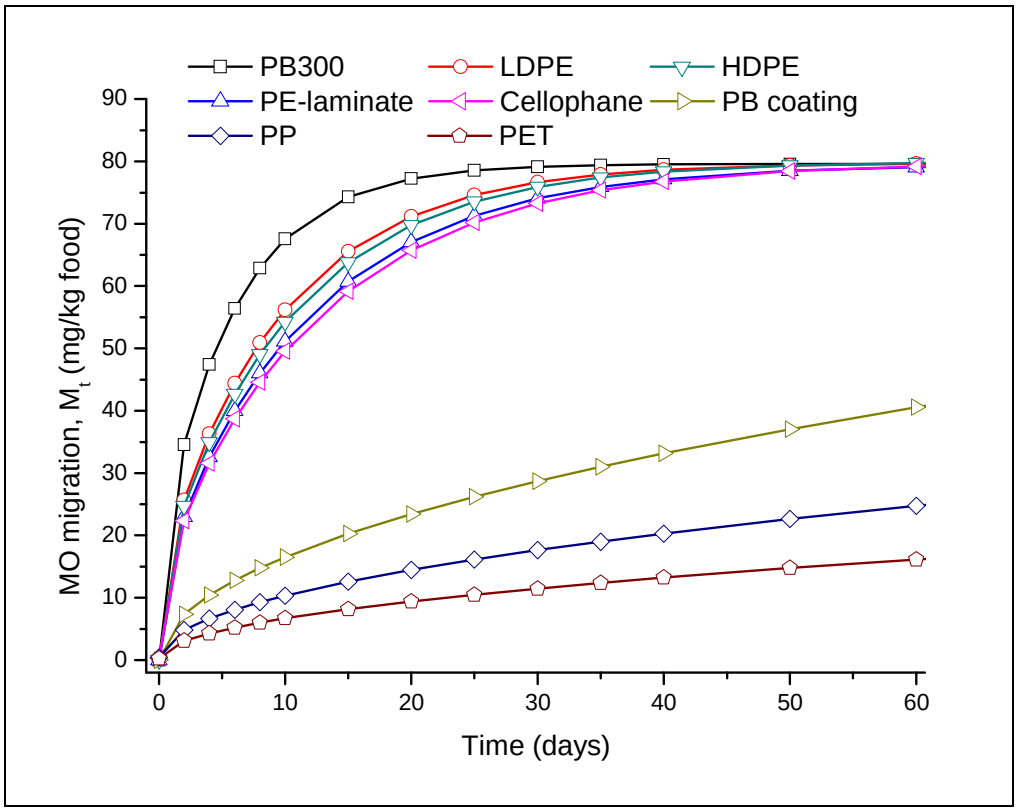

Figure 4.7: Predicted MO migration through model packaging materials.

4.6 Estimation of shelf-life

In order to estimate a reasonable shelf-life, the time at which the specific migration limit (SML) is reached could be obtained from the position on the y-axis where M_t = SML (Figure 4.7). Due to outstanding/insufficient toxicological data on MO for human consumption, the involved authorities have not yet reached consensus on a definite SML for MOSH or MOAH, and therefore no legal limit has yet been established. However, for purpose of illustration, the overall migration limit (OML) of 60 mg/kg will be used as a reference concentration to determine shelf-lives as derived from HVTR.

The shelf-lives determined from equation 4.15 and Figure 4.7, varied between 1 to 3 years for PP and PET respectively, about 6 months for barrier coated PB, and less than 1 month for poorer barriers. For uncoated PB, the concentration of 60 mg/kg food was reached within as little as 7 days. These shelf-lives are plotted against HVTR, and show an exponential dependence in Figure 4.8 (a). Due to large differences in shelf-lives of the tested materials, the logarithmic plot is shown for clarity in

Figure 4.8 (b) and illustrates a linear decrease of log(shelf-life) with increasing log(HVTR). Hence, for a given SML, the shelf-life of any value for HVTR can be calculated, and a simple table, such as presented in Table 4.4 of the shelf-life for different values of HVTR, may be used as a template to interpret HVTR results in a quick and easy way.

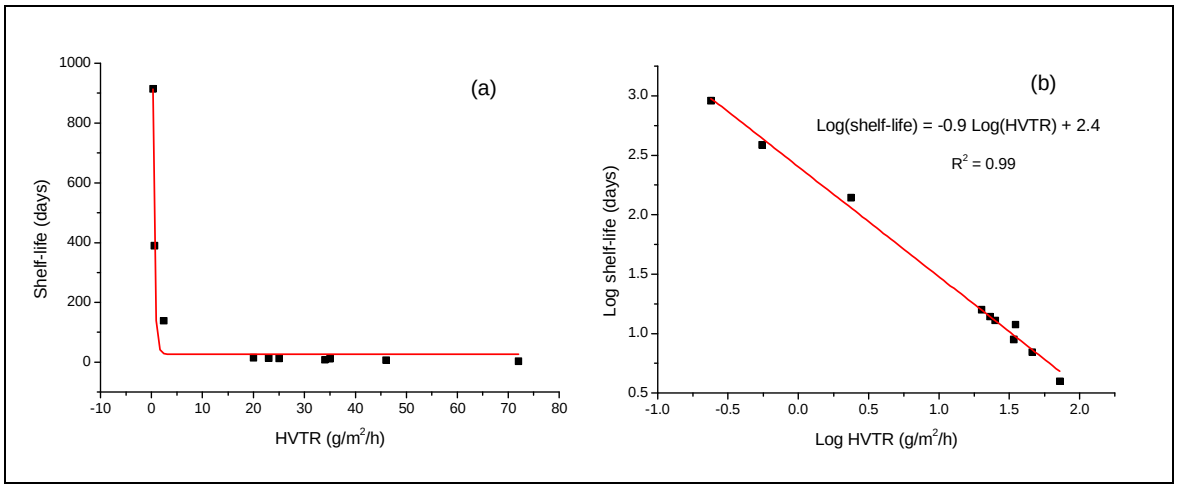

Figure 4.8: Shelf-life as a function of HVTR.

Table 4.4: Calculated shelf-life for different values obtained by HVTR

HVTR (g/m^2/h)	Shelf-life (days) SML = 60 mg/kg
0.2	1069
0.4	573
0.6	398
0.8	307
1	251
2	135
4	72
6	50
8	39
10	32
15	22
20	17
25	14

It can thus be concluded that from simplistic derivations from HVTR, a worst case shelf-life of the product–packaging combination could be determined, which is based on the diffusion coefficient of MO vapour through the packaging material, the thickness, as well as the initial concentration of MO in the packaging.

4.7 Validation

Repeatability studies of method validation for HVTR were carried out on at least 3 samples. The repeatability was estimated as the relative standard deviation (RSD) of penetrant in activated carbon, calculated by:

$$\frac{standard\ \ deviation}{average} \times 100 = RSD\ (\%) \qquad \textbf{Eq. 4.16}$$

RSD for HVTR measurements within 1 h varied between 2.5–12%, except for extremely good barriers with very little vapour mass uptake the RSD went up to 21%. However, apart from experimental errors associated with the method, the sensitivity of the balance contributes to 17% RSD for the lowest mass uptake measured. RSD for measurements done up to 8 h were between 0.5 and 6.5%, and good barriers had an RSD up to 10.5%. It is therefore recommended that for materials exhibiting low HVTR, the time of measurement is increased to more than 1 h. Differences in experimental data between samples could be attributed to disturbances in the heptane vapour saturated environment as a result of opening the sample chamber during weighing intervals.

4.8 Conclusions

A new method was successfully developed for the evaluation of organic vapour migration through paper and board intended to come into contact with food. The method was verified by measuring the permeation through various packaging substrates, which gave good agreement between MOVTR and HVTR. Since HVTR is a measure of heptane flux through the packaging materials, it was possible to derive the diffusion coefficient of MO (resembling real conditions of use, but still based on worst case scenarios) from Fick's first law. This enabled the migration modeling of MO over time, and in doing so accomplished the prediction of the shelf-life of the product. The advantage of this method is that it is quick, easy, and inexpensive, as opposed to conventional methods for measuring MO migration into a food simulant. The method described in this chapter can, therefore, be easily implemented as a quality control test in paper mills to monitor the efficiency of barrier coated boards in terms of the ability to protect food against contamination by MO and other related VOCs coming from the primary packaging, or even via secondary and tertiary packaging cross-contamination.

References

1. TAPPI T 559 cm-06 "Grease resistance test for paper and paperboard."
2. *TAPPI useful methods 1991*, TAPPI Press.
3. TAPPI T 462 cm-06 "Castor-oil penetration test for paper."
4. TAPPI T 454 om-06 "Turpentine test for voids in glassine and greaseproof papers."
5. TAPPI T 507 cm-09 "Grease resistance of flexible packaging materials."
6. ASTM F 119–82 "Rate of grease penetration of flexible barrier materials (Rapid method)." ASTM International.
7. Krohn, J. V. and Jordy, D. W., A comparison of the oil, oxygen, and water-vapor permeation rates of various polyethylene blown films. *TAPPI J.,* (1997) 80: 151–156.
8. Crank, J. and Park, G. S., *Diffusion in Polymers*, Academic Press, London, 1968.
9. Shepherd, A., Activated carbon adsorption for treatment of VOC emissions. *13th Annual EnviroExpo*, *2001*. Boston Massachusetts.
10. Diaz, E., Ordonez, S., Vega, A., and Coca, J., Adsorption characterisation of different volatile organic compounds over alumina, zeolites and acitivated carbon using inverse gas chromatography. *J. Chromatogr. A,* (2004) 1049: 139–146.
11. Kim, K.-J., Kang, C.-S., You, Y.-J., Chung, M.-C., Jeong, S. W., Jeong, W.-J., Woo, M.-W., and Ahn, H.-G., Adsorption-desorption characteristics of modified activated carbons for volatile organic compounds. *Stud. Surf. Sci. Catal.,* (2006) 159: 457–460.
12. Lillo-Rodenas, M. A., Cazorla-Amoros, D., and Linares-Solano, A., Behaviour of activated carbons with different pore size distributions and surface oxygen groups for benzene and toluene adsorption at low concentrations. *Carbon,* (2005) 43: 1758–1767.
13. Aurela, B. and Ketoja, J. A., Diffusion of volatile compounds in fibre networks: experiments and modelling by random walk simulation. *Food Addit. Contam.,* (2002) 19: 56–62.
14. Pocas, M. d. F., Oliveira, J. C., Pereira, J. R., Brandsch, R., and Hogg, T., Modelling migration from paper into a food simulant. *Food Control,* (2011) 22: 303–312.
15. Vollmer, A., Biedermann, M., Grundbock, F., Ingenhoff, J.-E., Biedermann-Brem, S., Altkofer, W., and Grob, K., Migration of mineral oil from printed paperboard into dry foods: survey of the German market. *Eur. Food Res. Technol.,* (2011) 232: 175–182.
16. Hampe, D. and Piringer, O., Studies on the permeation of inorganic salts through plastic films. *Food Addit. Contam.,* (1998) 15: 209–216.

17. Zulch, A. and Piringer, O., Measurement and modelling of migration from paper and board into foodstuffs and dry food simulants. *Food Addit. Contam.,* (2010) 29: 1306–1324.

18. Haylett, D. R., Davidson, D. F., and Hanson, R. K., Ignition delay times of low-vapor-pressure fuels measured using an aerosol shock tube. *Combust. Flame,* (2012) 159: 552–561.

19. Crank, J., *The Mathematics of Diffusion*, 2nd ed, Clarendon Press, Oxford, 1975.

20. Piringer, O., Franz, R., Huber, M., Begley, T. H., and McNeal, T. P., Migration from food packaging containing a functional barrier: mathematical and experimental evaluation. *J. Agr. Food Chem.,* (1998) 46: 1532–1538.

21. Begley, T., Castle, L., Feigenbaum, A., Franz, R., Hinrichs, K., Lickly, T., Mercea, P., Milana, M., O'Brien, A., Rebre, S., Rijk, R., and Piringer, O., Evaluation of migration models that might be used in support of regulations for food-contact plastics. *Food Addit. Contam.,* (2005) 22: 73–90.

22. Rosca, I. D. and Vergnaud, J.-M., Approach for a testing system to evaluate food safety with polymer packages. *Polym. Test.,* (2006) 25: 532–543.

23. Koontz, J. L., Moffitt, R. D., Marcy, J. E., O'Keefe, S. F., Duncan, S. E., and Long, T. E., Controlled release of a-tocopherol, quercetin, and their cyclodextrin inclusion complexes from linear low-density polyethylene (LLDPE) films into a coconut oil model food system. *Food Addit. Contam.,* (2010) 27: 1598–1607.

24. Brandsch, J., Mercea, P., Ruter, M., Tosa, V., and Piringer, O., Migration modelling as a tool for quality assurance of food packaging. *Food Addit. Contam.,* (2002) 19: 29–41.

25. Cruz, J. M., Silva, A. S., Garcia, R. S., Franz, R., and Losada, P. P., Studies of mass transport of model chemicals from packaging into and within cheeses. *J. Food Eng.,* (2008) 87: 107–115.

26. *Industry guideline for the compliance of paper and board materials and articles for food contact*, in http://www.cepi.org. March, 2010.

Chapter 5

Sorption of model packaging materials

5.1 Introduction

Sorption and transport of organic vapours in a wide range of materials have been studied for various reasons, for example:

- To evaluate the ability of a membrane to separate VOC pollutants from air [1];
- To predict the electrical performance of conductive composites (carbon black filled polyurethane) when exposed to VOCs [2];
- To compare the barrier properties of different materials towards VOCs [3];
- To determine the effect of morphological differences such as degree of crystallinity on VOC diffusion [4].

Transport of gases and vapours through polymers is an important aspect in food packaging applications. Therefore, a better understanding of transport mechanisms in packaging materials is necessary in order to achieve significant improvements in barrier properties. Different types of methods for studying transport properties of polymer films are available, namely permeation, sorption, and pervaporation [5]. These methods allow the determination of a material's permeability towards gases or vapours. Permeability of packaging materials plays an important role in the shelf-life of a product. Testing foodstuffs under actual storage conditions are a long-term process and often a costly procedure. Therefore, the permeability coefficient of a material is necessary for the theoretical prediction of shelf-life, which is also more practical and less time consuming than migration studies under real conditions.

Transport parameters of a material depend on a number of factors, such as temperature, type of penetrant, penetrant activity, and the physico-chemical properties of the polymeric membrane [5, 6]. Friess and co-workers compared the transport properties of polymer membranes as determined by both permeation and sorption experiments [7, 8]. The permeability coefficients (P) as determined from permeation (steady-state conditions) showed good agreement with P as determined from sorption data (equilibrium uptake), given that the membranes exhibited relatively low vapour sorption properties. They showed the possibility of using only one of the experimental methods for estimating

permeability coefficients, without the need to perform the other method. However, for membranes and vapour combinations with high sorption properties, P was found to be higher when determined from sorption experiments than from permeation experiments. They also found a good correlation of the solubility coefficients obtained from both methods, where S was directly determined from sorption measurements, and calculated from the solution-diffusion model (P = D x S) from permeation experiments.

In this study, the permeability coefficients as determined from both permeation and sorption experiments were compared, in order to determine whether results from the permeation method at atmospheric pressure were sufficient to predict material behaviour at low partial pressure. Furthermore, sorption behaviour studied over a wide range of penetrant partial pressures offers essential information on materials in terms of their barrier properties towards mineral oils.

5.2 Results and discussion

5.2.1 Sorption isotherms

n-Heptane sorption measurements were carried out at 23℃, and a range of vapour partial pressures from 0.01 to 0.9. The partial pressure is expressed as p/p_0, where p is the actual pressure of an atmosphere containing only heptane vapour, and p_0 is the saturation vapour pressure of *n*-heptane, at 23℃ (i.e. 54.946 mbar). A sorption isotherm report s on the maximum penetrant uptake by a material when equilibrium is reached, for a wide range of partial pressures, typically from 0 to 1. Each point on the isotherm graph is accordingly obtained from one sorption experiment, as shown in Figure 5.1 by mass uptake = f(t), at a specific partial pressure and temperature (i.e. 23℃), with the mass uptake determined from infinite time being reported in the sorption isotherms. Sorption isotherms at 23℃ are given in Figure 5.2. Measurements revealed that LDPE exhibited the highest % mass uptake at all partial pressures, and PET the lowest when sorption equilibrium was reached. Total heptane mass uptake at equilibrium were found in the order LDPE > PP > cellophane > HDPE > PET. Most sorption isotherms appear to have a linear Henry-type dependence of mass uptake vs. p/p_0, up to a heptane partial pressure of 0.7. At higher vapour activities (p/p_0 > 0.7), a Flory-Huggins shape convex to the *x*-axis was generally observed, also known as BET type III sorption isotherms. These trends are in agreement with literature [9-11], and indicate that polymer-polymer interactions prevail in the low

partial pressure range, whereas penetrant-penetrant interaction has a larger effect for high partial pressures.

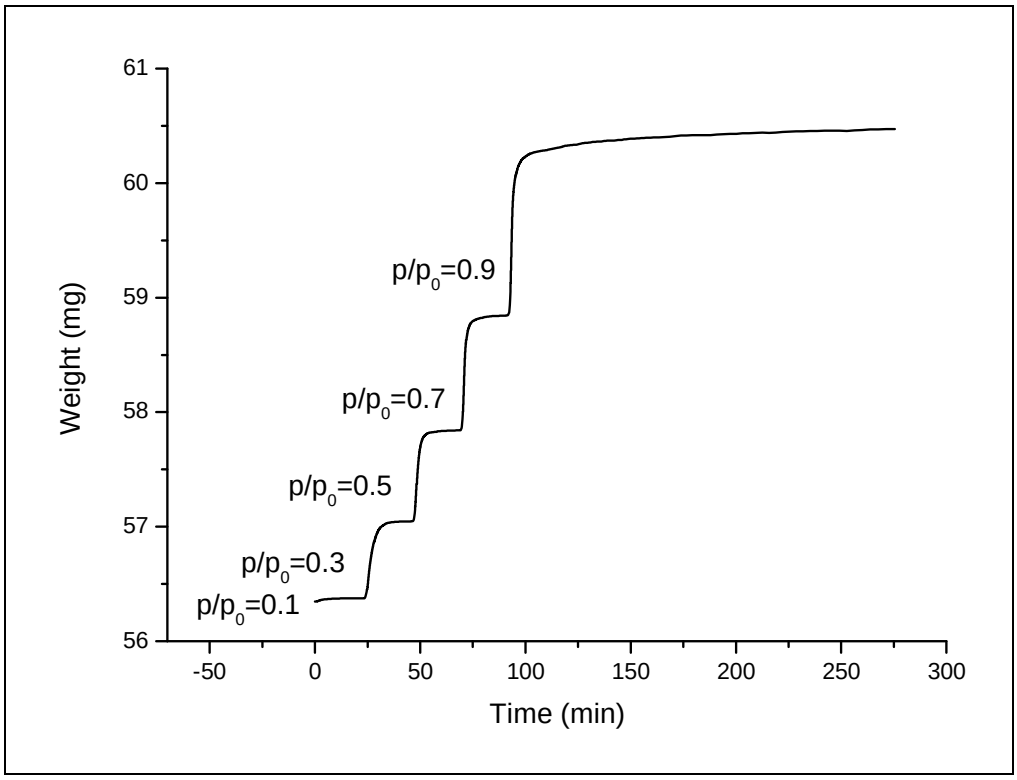

Figure 5.1: A set of sorption experiments of mass uptake as a function of time, at different partial pressures.

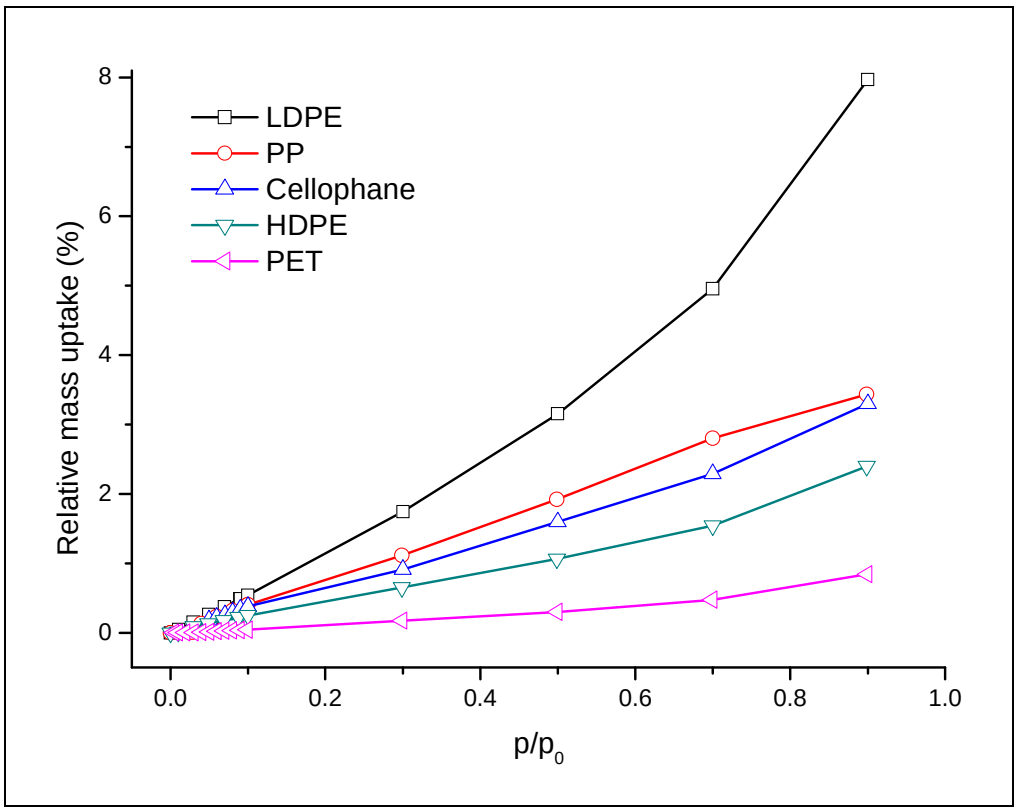

Figure 5.2: Sorption isotherms of various packaging films in heptane vapour.

It should be mentioned that PP was the only material tested that did not reach equilibrium in the maximum time-out measurement set to 40 h. This lead to an underestimation of the heptane mass uptake throughout the entire range of partial pressures in the subsequent sorption isotherm. This can be also be seen by the typical kinetic plot of mass uptake ratio as a function of $\sqrt{t}$, and an example at p/p_0 = 0.7 is shown in Figure 5.3. *n*-heptane uptake by PP appears to be increasing slowly but steadily, similar to sorption of other organic vapours such as benzaldehyde in PP that showed slow uptake even up to 150 h exposure time over the partial pressure range 0.3–0.9 [11]. This was attributed to the organic penetrant acting as a plasticiser in the polymer, thereby allowing changes in the polymer morphology such as redistribution of free volume and crystalline regions. Also, polymer films often contain internal stresses as a result of processing conditions (for example rapid cooling after thermal treatment), which can slowly alleviate upon interaction with the organic penetrant.

Furthermore, the kinetic behaviour provided a deeper understanding of the potential barrier properties of each of the materials as obtained by HVTR. LDPE illustrated rapid heptane vapour uptake, together with a high equilibrium mass uptake, and both factors contributing to a relatively high HVTR of ~35 g/m^2/h. HDPE, on the other hand, did not exhibit the same high equilibrium mass uptake, but the

rate of heptane uptake was just as fast (HVTR ~25 g/m^2/h). Cellophane and PP, which had lower HVTR values (~20 and ~0.5 g/m^2/h respectively) than the polyethylenes, each illustrated a higher equilibrium mass uptake than HDPE, yet their rate of heptane uptake as displayed in Figure 5.3 was found to be much slower. PET had the lowest equilibrium and rate of heptane uptake.

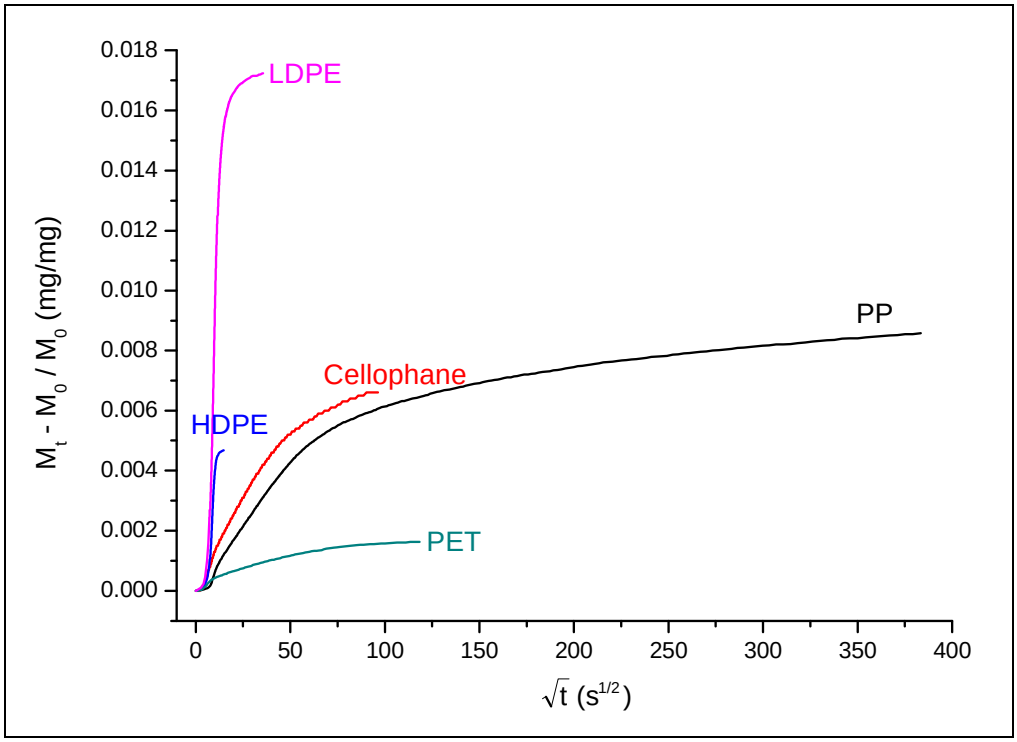

Figure 5.3: Sorption kinetic plots at $p/p_0 = 0.7$, T = 23℃.

5.2.2 Transport coefficients

The transport coefficients, i.e. permeability coefficient (P), diffusion coefficient (D), and solubility coefficient (S), were calculated as explained in Chapter 3 (section 3.2.4), and the values are given in Table 5.1.

Table 5.1: Transport parameters of model packaging materials

	PET			PP			Cellophane			HDPE			LDPE		
p/p_0	S[#]	D[⌘]	P[§]	S	D	P	S	D	P	S	D	P	S	D	P
0.01	–	–	–	–	–	–	–	–	–	–	–	–	21.24	57.11	121
0.03	–	–	–	–	–	–	–	–	–	27.88	3.22	8.99	23.23	66.73	155
0.04	2.31	17.76	4.09	24.08	0.27	0.65	–	–	–	–	–	–	–	–	–
0.05	2.64	18.20	4.80	–	–	–	16.21	0.17	0.28	25.70	9.37	24.09	24.30	66.61	161
0.06	2.89	22.96	6.66	27.59	0.38	1.04	16.57	0.26	0.44	–	–	–	–	–	–
0.07	3.01	30.80	9.27	–	–	–	16.37	0.39	0.64	24.20	13.60	32.92	24.69	77.86	192
0.08	3.12	30.60	9.55	28.28	0.16	0.44	16.43	0.37	0.61	–	–	–	–	–	–
0.09	3.17	30.36	9.64	–	–	–	16.81	0.23	0.39	23.31	24.48	57.05	24.99	79.89	199
0.1	4.43	22.50	9.97	28.53	0.20	0.58	16.68	0.37	0.61	–	–	–	25.01	119.22	298
0.3	4.51	30.40	13.70	26.27	0.51	1.34	13.53	0.30	0.41	20.39	20.43	41.65	26.74	133.30	356
0.5	4.53	34.50	15.61	27.20	1.33	3.63	14.33	0.74	1.06	20.04	22.25	44.59	29.11	247.81	721
0.7	4.94	42.20	20.85	28.34	3.06	8.68	14.59	3.15	4.60	21.00	30.15	63.32	32.56	342.45	1115
0.9	6.73	37.60	25.29	27.01	60.20	162.60	16.32	10.86	17.72	25.26	13.00	32.84	40.75	291.17	1186

S x 10^2, cm^3(STP)/cm.mbar
⌘ D x 10^{10}, cm^2/s
§ P x 10^{11}, cm^3(STP)cm/cm^2.s.mbar

Plots of the diffusion coefficients, D, as a function of partial pressure are given in Figure 5.4. It was found that LDPE exhibited a much higher diffusion coefficient as compared to all other materials tested. A statistical evaluation of diffusion coefficients of different polymers used in food contact applications also revealed that LDPE has one of the highest diffusion coefficients [10]. Diffusion coefficients were generally in the order LDPE > PET > HDPE > PP > cellophane, and were found to increase with increasing partial pressure up to p/p_0 of 0.7. However, a drop of the diffusion coefficient was then observed at p/p_0 = 0.9 for LDPE, PET and HDPE. A similar effect was observed by Friess et al. [9] who concluded that it was not caused by changes in the crystallinity of the material, but rather caused by the molecular aggregation of penetrant molecules at high concentration. The reduction in D can, therefore, be explained by clustering of heptane vapour molecules at high partial pressures, thus leading to a lower molecular mobility in the polymer films. This is characterised by predominant penetrant-penetrant interactions which are found for materials with a typical Flory-Huggins type sorption isotherm [6], as also shown in Figure 5.2. However, the effect of clustering did not influence the diffusion of heptane in PP or cellophane.

The trend in diffusion coefficients obtained from HVTR measurements were found to be different than the trends obtained from sorption measurements. PET illustrated quite high diffusion coefficients over the range of partial pressures, as compared to HDPE, PP, and cellophane, which can in the first place seem contradictory that PET was found to be the best barrier to MO according to the HVTR test method. However, the reason for this is reflected in the solubility coefficients obtained from heptane sorption experiments.

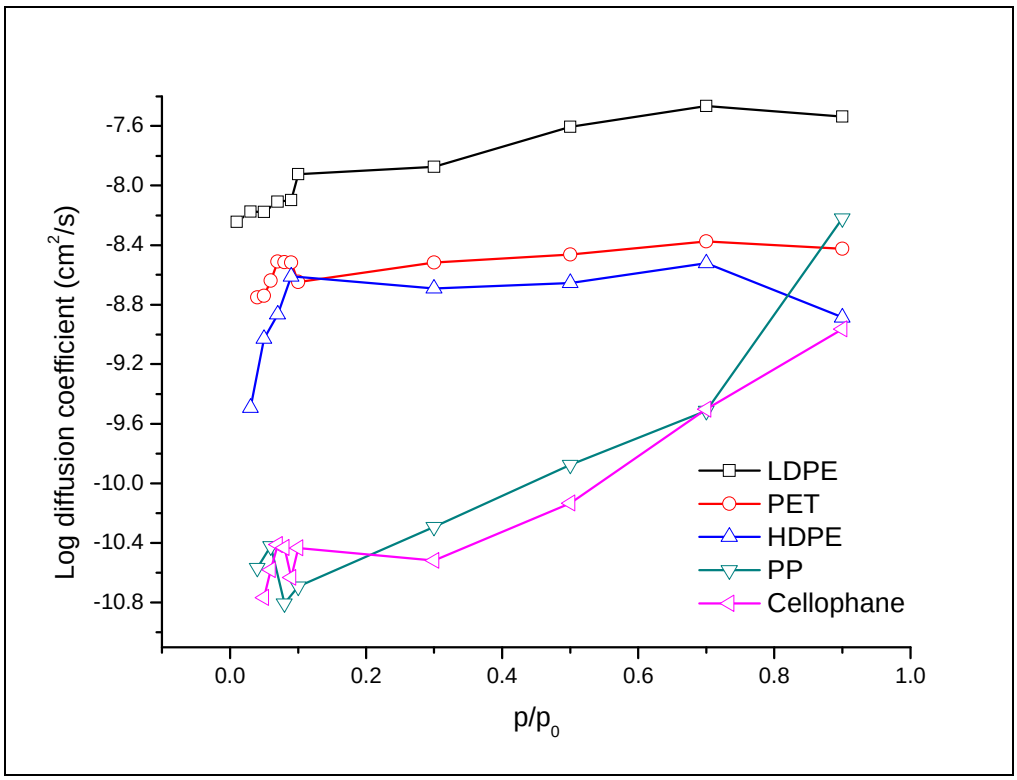

Figure 5.4: Diffusion coefficients of heptane in polymer films at increasing partial pressure.

Solubility coefficients determined from sorption experiments are plotted as a function of p/p_0 in Figure 5.5. PET illustrated the lowest solubility coefficients across the tested pressure range, and could explain why even though PET exhibit relatively fast diffusion of heptane, the overall permeability as found with HVTR remains lower than for the other tested materials. The highest solubility coefficients were obtained for LDPE, HDPE, and PP, showing that the polyolefins had higher affinities towards heptane vapour, as a higher number of penetrant molecules were sorbed onto these polymer films.

For cellophane, PP, and HDPE, the solubility coefficients were found to be fairly independent from the partial pressure. For LDPE and PET an increase of the solubility coefficients were observed with increasing partial pressure, showing that the solubility of heptane, and therefore also MO, will depend on the concentration of the contaminant in these packaging materials. The solubility coefficients for various materials decreased in the following order: LDPE > PP > HDPE > cellophane > PET.

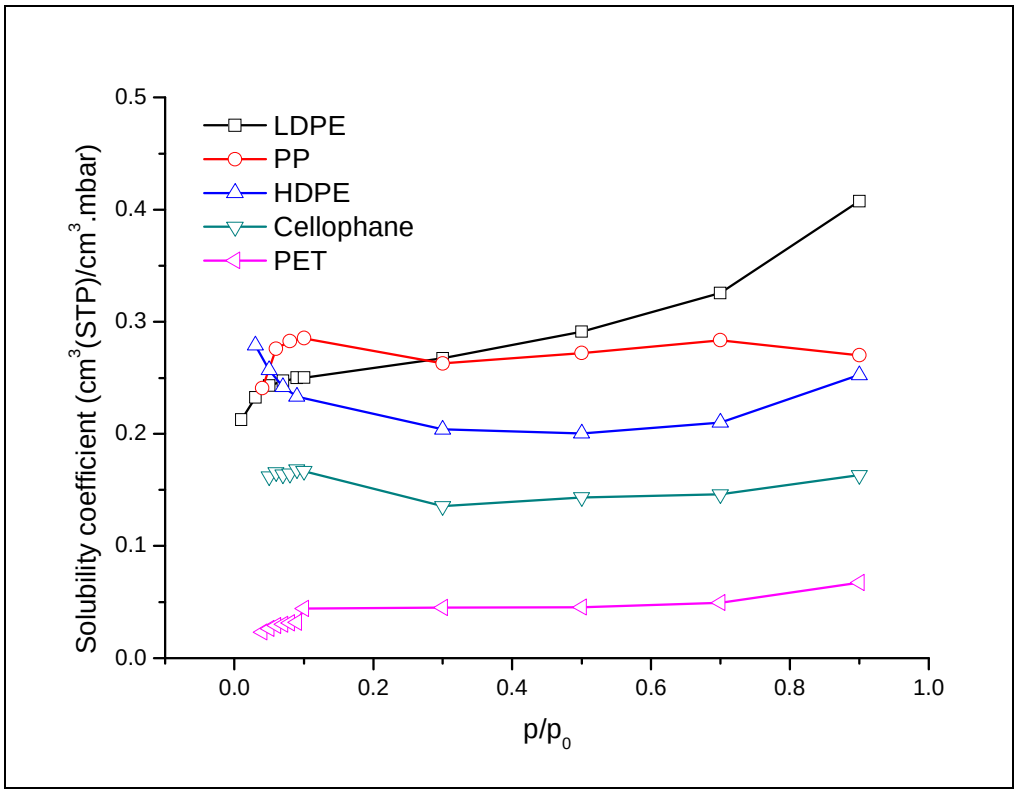

Figure 5.5: Solubility coefficients of heptane in model packaging films at increasing partial pressure.

Plots of P as a function of p/p_0 (Figure 5.6) revealed that the permeability of cellophane, PP, and HDPE are controlled mostly by kinetic factors (i.e. diffusion coefficients), as the thermodynamic parameters (i.e. solubility coefficients) remains largely unaffected by heptane concentration. For LDPE and PET, the change in the solubility coefficient of heptane vapour with p/p_0 played a more significant role in permeability, which was evident at high partial pressures. As examples, Figure 5.7 illustrates the dominant effect D has on permeability of PP, and similar tendencies were obtained for HDPE and cellophane. Figure 5.8, on the other hand, shows an increasing trend between P, D, and S of LDPE as p/p_0 increase up to 0.7, but at high p/p_0 it becomes evident that the overall permeability is not controlled by diffusion only, as P increase while D decrease.

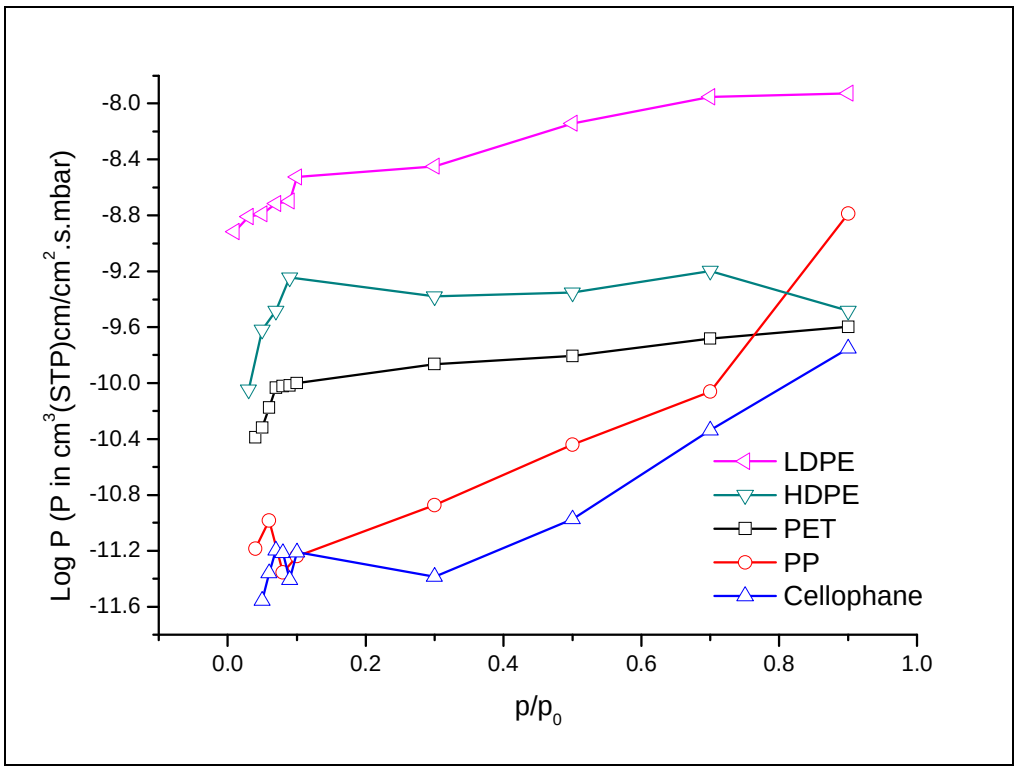

Figure 5.6: Permeability coefficients of heptane in model packaging films at increasing partial pressure.

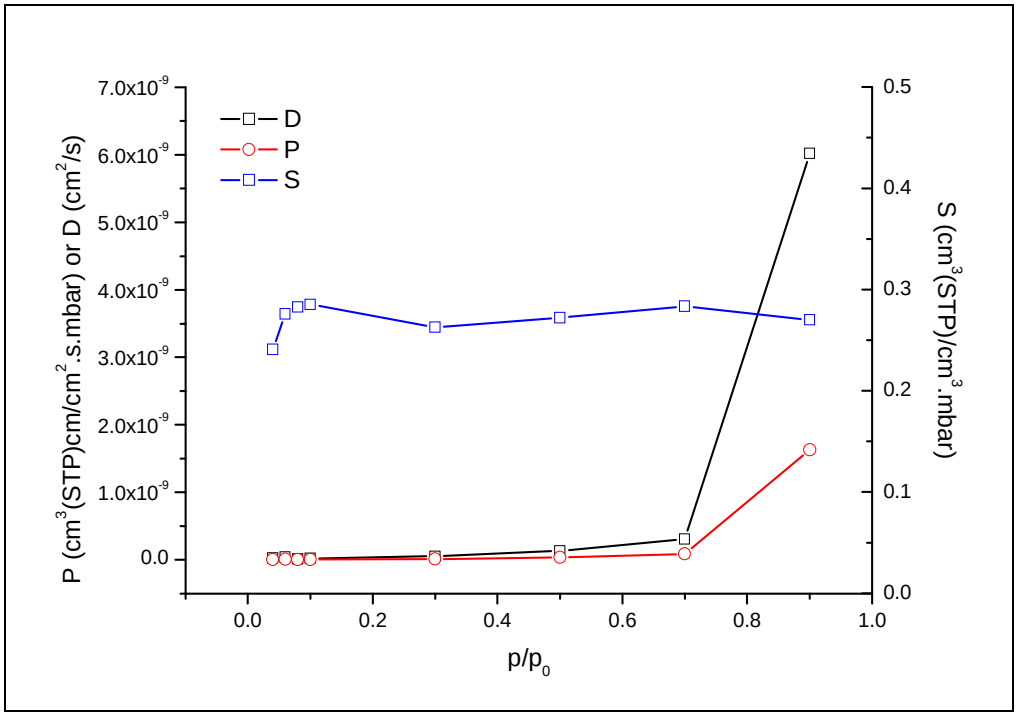

Figure 5.7: Permeability coefficient (P), diffusion coefficient (D), and solubility coefficient (S) for various partial pressures of heptane for PP substrate.

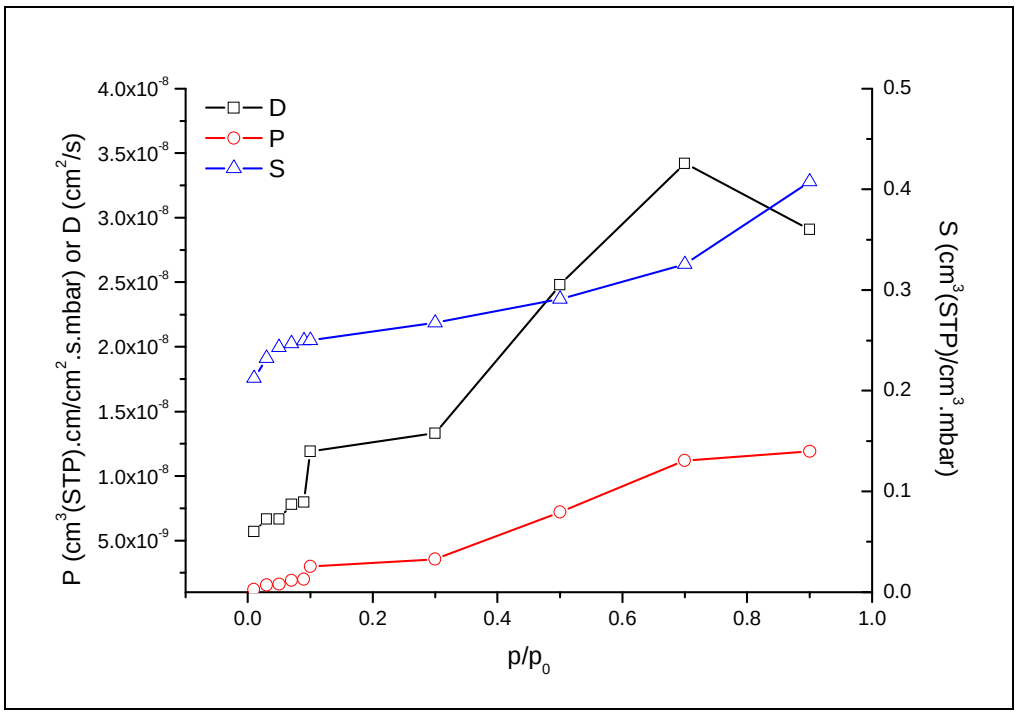

Figure 5.8: Permeability coefficient (P), diffusion coefficient (D), and solubility coefficient (S) for various partial pressures of heptane for LDPE substrate.

These figures indicate that transport of heptane is mostly controlled by diffusion. This verifies that the model used in Chapter 4, section 4.5 and 4.6, where the shelf-life predictions were based on the estimated diffusion coefficients of MO in model packaging materials, is an appropriate model for migration predictions under real conditions of use.

5.2.3 Polymer-penetrant interaction

Several models are available in the literature to describe gas or vapour sorption isotherms in polymers. Some common models were utilised to give more insight into polymer-penetrant interactions of the model packaging materials with heptane vapour, i.e. *Engaged Species Induced Clustering* (ENSIC) model which is an extension of the Flory-Huggins theory, three-parameter Brunauer-Emmett-Teller (BET), Guggenheim-Anderson-de Boer (GAB), and a modified dual mode sorption (DMS) model. The BET [12] and DMS [13] models used in this study provided good fits to the experimental data, mainly because these two models are known to describe best the sorption isotherms of BET II type isotherms, which are typically concave to the *x*-axis at low partial pressure, and convex at high partial pressure, giving a sigmoidal shape to the isotherm. Originally, the isotherms appeared to follow BET type III behaviour as identified in Figure 5.2. However, the poor fit of the ENSIC model which

usually describe these sorption isotherms quite well [14], revealed a slight concave tendency in the isotherms to the *x*-axis at low partial pressure, thus displaying BET II type isotherms.

The DMS model resulted in the best fit to the heptane vapour sorption isotherms of all the tested materials, and is given by the relationship [13]:

$$c = C_P \frac{ka}{1-ka} + C_P \frac{(A-1)ka}{1+(A-1)ka} \qquad \textbf{Eq. 5.1}$$

where c is the penetrant concentration in the polymer, a is the penetrant activity, C_P is the sorption capacity of a polymer to a penetrant, k is the ratio of the partition function of molecules sorbed in the multilayer to that of molecules in the bulk liquid (indicating the difference between the interaction of penetrant molecules and penetrant-polymer interaction), and A is the ratio of the partition function of the first molecule sorbed on a site to that of molecules sorbed beyond the first molecules in the multilayer. Even though this model was developed to describe vapour sorption in glassy polymers, in which dual refers to the two types of vapour sorption sites (i.e. the matrix region of the glassy polymer, and the microvoids present in glassy polymers), it has also been shown to be applicable to vapour sorption in rubbery [13] and semi-crystalline [15] polymers.

This DMS relationship was applied to the experimental data obtained by heptane vapour sorption experiments, and obtained curves are shown in Figure 5.9. Data fitting was done by non-linear regression, based on the Levenberg-Marquardt algorithm as employed by Origin V8 software. DMS model parameters as well as statistical factors are given in Table 5.2. The reduced chi-square value indicates the mean deviation of each fitted data point from the experimental data, and R^2 is a correlation factor indicating the efficiency of the fit. The A-parameter may be used to explain the state of the polymer, since $A < 1$ is indicative of glassy behaviour with sorption in microvoids, whereas $A \geq 1$ indicates rubbery behaviour, which was the case for all materials tested. The k-values can vary from 0 to 1, 0 indicating poor interaction between penetrant and polymer, and 1 indicating the strongest interaction. Surprisingly, this value was the highest for PET, lower for the polyethylenes, and even lower for cellophane. C_P, on the other hand, shows that PET has the lowest sorption capacity towards heptane vapour, and LDPE the highest.

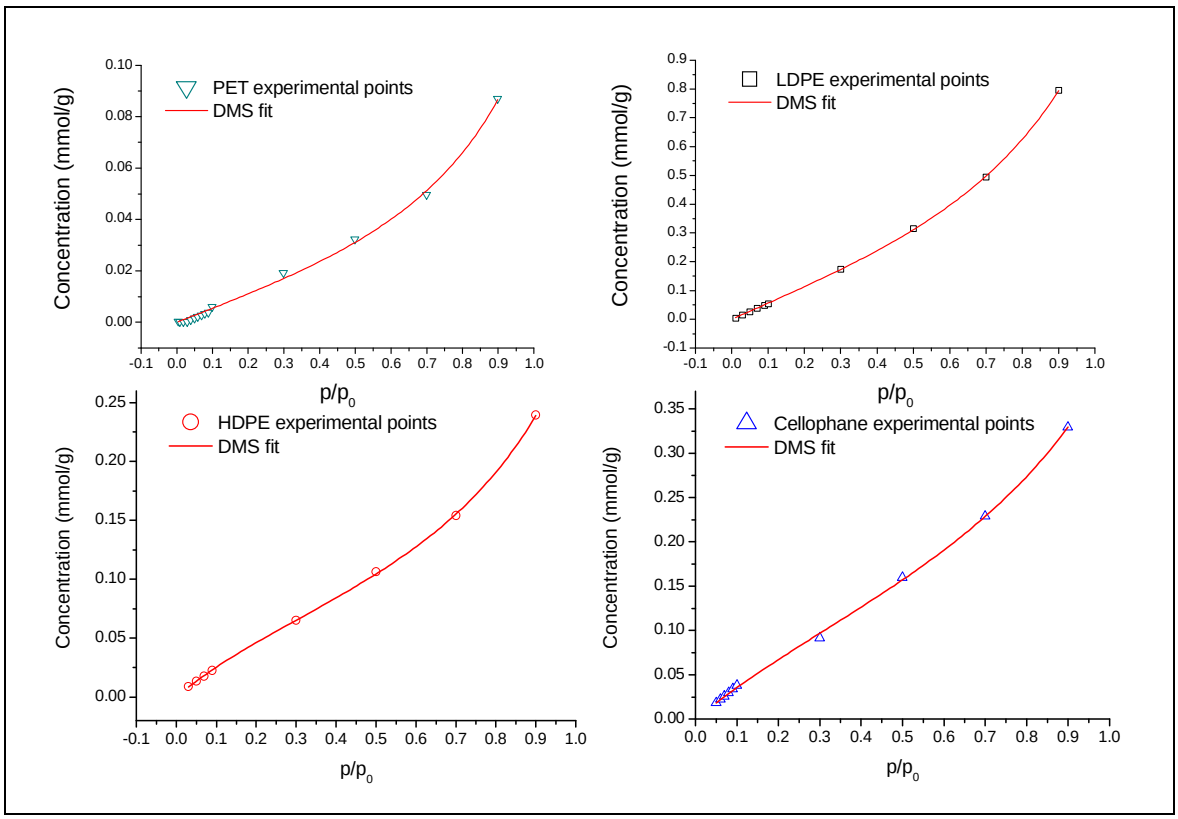

Figure 5.9: DMS model fit to heptane vapour isotherms of PET, LDPE, HDPE, and cellophane.

Table 5.2: DMS model parameters of model packaging materials

Material	DMS model parameters						Statistical correlation	
	C_P	Std error	k	Std error	A	Std error	Reduced φ^2	R^2
PET	0.035	0.006	0.746	0.037	2.099	0.473	1.56×10^{-6}	0.997
Cellophane	0.175	0.012	0.627	0.021	3.509	0.272	6.44×10^{-6}	0.999
LDPE	0.388	0.016	0.691	0.009	2.095	0.104	5.17×10^{-6}	0.999
HDPE	0.095	0.003	0.720	0.009	4.245	0.225	1.12×10^{-6}	0.999

5.2.4 Comparison of permeability coefficients from sorption and permeation

Permeability coefficients as experimentally determined from the permeation test method, P_{perm}, at a saturated heptane vapour environment at atmospheric pressure, i.e. p/p_0=0.05, were compared to the permeability coefficients as calculated over the pressure range 0.01–0.9 via gravimetric sorption, P_{sorp}. P_{perm} and P_{sorp} are shown in Figures 5.10, a–d. For each of the tested materials, P_{perm} was found to be much higher than P_{sorp}. The same outcome has been published previously where permeability determined via sorption experiments was underestimated as compared to permeability measured by permeation experiments [16]. The reason lies in the difference between the experimental conditions of the two methods as detailed below.

The permeation method is carried out in atmospheric pressure of saturated heptane vapour in air, hence containing mostly oxygen and nitrogen. This may contribute to an enhanced permeation, where supplementary gases in the heptane environment may facilitate the heptane migration through the packaging materials. It has also been reported in the literature that the presence of additional gases could increase the rate of transfer of a selected penetrant through a polymer film [16]. For example, it is commonly known that the presence of moisture vapour in polymer films can enhance the oxygen transmission rates (OTR). This is mainly observed for hydrophilic type polymers where significant interaction between the polymer and moisture vapour enhances OTR. However, OTR of hydrophobic polymers such as HDPE and LDPE is not affected by the presence of moisture [17]. Therefore, it is believed that since the two main components present in the HVTR method, O_2(g) and N_2(g), is also non-polar gases as is heptane, the poorer heptane (and thus MO) barriers will be more affected by the presence of the additional gases than the good barriers. When P_{sorp} and P_{perm} at p/p_0 = 0.05 was compared, it was found that P_{perm} was larger for all materials by a factor of 10, except for cellophane where P_{perm} was roughly 3 orders of magnitude higher. Since cellophane is polar in nature, it is reasonable to conclude that the presence of the non-polar gases could contribute to higher permeability coefficients as obtained with permeation.

Nonetheless, permeability coefficients determined by permeation proved to resemble a “worst case scenario”, giving the highest values for P, and also being a closer resemblance to real conditions of storage and use, as compared to sorption experiments carried out under vacuum controlled conditions. Based on these findings, the derivations made from the HVTR method predicted a safe margin for shelf-life determination in terms of MO barrier properties.

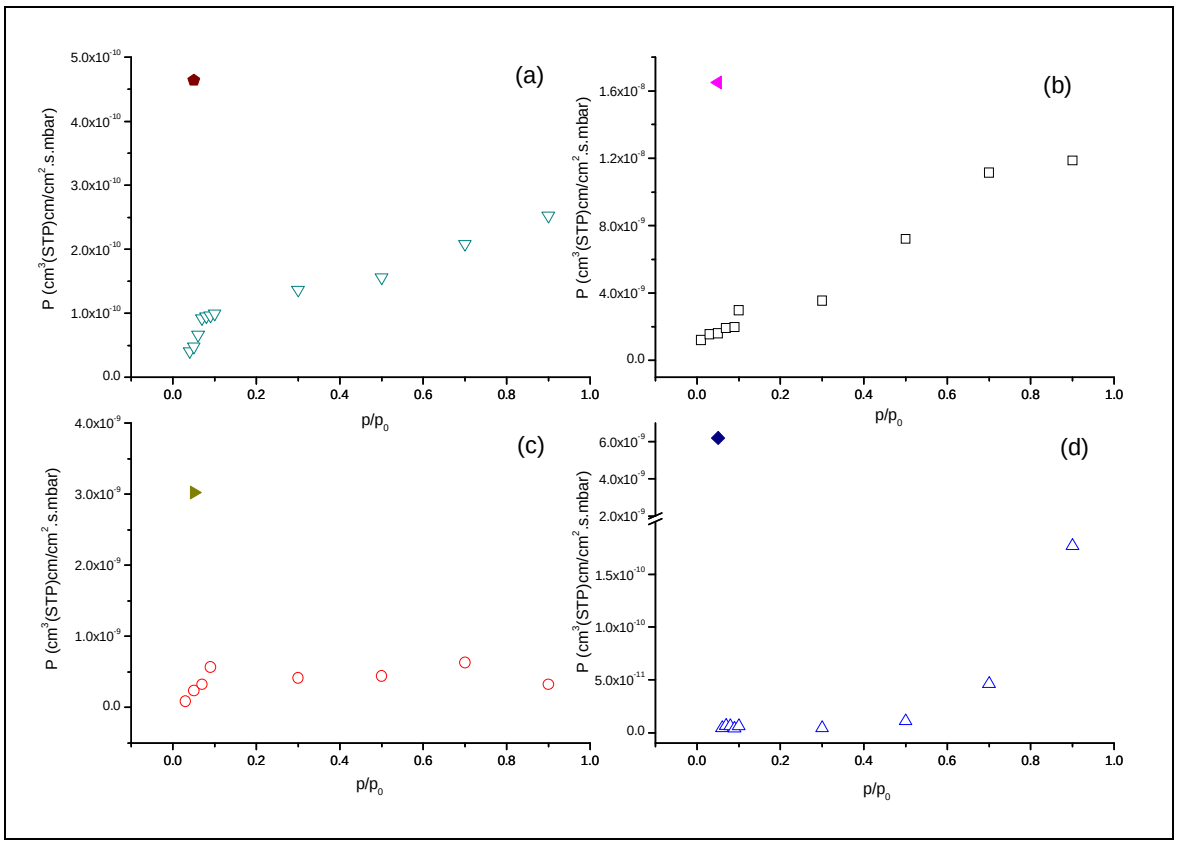

Figure 5.10: Permeability coefficients determined by sorption experiments (open symbols) between p/p_0 = 0.01–0.9, and permeation experiments (solid symbols) at p/p_0 = 0.05 of (a) PET, (b) LDPE, (c) HDPE, and (d) cellophane.

5.3 Conclusions

Sorption data allowed a more profound understanding of the interaction between the respective model polymeric films and heptane vapour. Isotherms revealed that not only did the equilibrium mass uptake play a role in the ability of the model packaging materials to behave is a MO barrier, but also the rate of uptake obtained from the sorption kinetics. A comparison of the transport coefficients, P, D, and S, over a wide range of penetrant partial pressures showed that the migration of volatile organic compounds through the model polymeric films was mostly controlled by diffusion, although for some materials a more pronounced effect was observed by the solubility coefficient. Sorption behaviour of the tested materials fitted well to a modified dual mode sorption model. The DMS model parameters could thus be used to acquire insight into the ability of a materials to perform as a MO barrier, which could also be useful during product development of MO barriers. Findings from a comparison between the permeability coefficients as obtained by the two different test methods, permeation and gravimetric sorption experiments, showed that the permeability coefficient could be underestimated by sorption

over the entire range of partial pressures tested. The permeability coefficients obtained from permeation experiments at a single penetrant partial pressure, at atmospheric pressure, was always higher than that obtained by sorption experiments performed under high vacuum. This was evidence that the predictions made in Chapter 4 from HVTR results were reasonable in that it constitutes a "worst case scenario."

Information obtained from sorption experiments provided valuable information about the interactions of organic vapour simulant with different polymers, which could be required in the development of new MO barrier materials. Nevertheless, the newly developed HVTR test method provides sufficient information to approximate real-life conditions, thereby contributing to understanding the barrier properties of packaging materials towards MO vapour.

References

1. Nguyen, Q. T., Langevin, D., Bahadori, B., Callebert, F., and Schaetzel, P., Sorption and diffusion of volatile organic components in a membrane made by deposition of tetramethyl disiloxane in cold remote-plasma. *J. Membrane Sci.,* (2007) 299: 73–82.
2. Zhao, B., Fu, R. W., Zang, M. Q., Zang, B., Zeng, W., Rong, M. Z., and Zheng, Q., Analysis of gas sensing behaviors of carbon black/waterborne polyurethane composites in low concentration organic vapor. *J. Mater. Sci.,* (2007) 42: 4575–4580.
3. Herrera-Alonso, J. M., Marand, E., Little, J., and Cox, S. S., Polymer/clay nanocomposites as VOC barrier materials and coatings. *Polymer,* (2009) 50: 5744–5748.
4. Lutzow, N., Tihminlioglu, A., Danner, R. P., Duda, J. L., Haan, A. D., Warnier, G., and Zielinski, J. M., Diffusion of toluene and n-heptane in polyethylenes of different crystallinity. *Polymer,* (1999) 40: 2797–2803.
5. George, S. C. and Thomas, S., Transport phenomena through polymeric systems. *Prog. Polym. Sci.,* (2001) 26: 985–1017.
6. Klopffer, M. H. and Flaconneche, B., Transport properties of gases in polymers: bibliographic review. *Oil Gas Sci. Technol.,* (2001) 56: 223–244.
7. Friess, K., Sipek, M., Hynek, V., Sysel, P., Bohata, K., and Izak, P., Comparison of permeability coefficients of organic vapors through non-porous polymer membranes by two different experimental techniques. *J. Membrane Sci.,* (2004) 240: 179–185.
8. Friess, K., Hynek, V., Sipek, M., Kujawski, W. M., Vopicka, O., Zgazar, M., and Kujawski, M. W., Permeation and sorption properties of poly(ether-block-amide) membranes filled by two types of zeolites. *Sep. Purif. Technol.,* (2011) 80: 418–427.
9. Friess, K., Jansen, J. C., Vopicka, O., Randova, A., Hynek, V., Sipek, M., Bartovska, L., Izak, P., Dingemans, M., Dewulf, J., Langenhove, H. v., and Drioli, E., Comparative study of sorption and permeation techniques for the determination of heptane and toluene transport in polyethylene membranes. *J. Membrane Sci.,* (2009) 338: 161–174.
10. Begley, T., Castle, L., Feigenbaum, A., Franz, R., Hinrichs, K., Lickly, T., Mercea, P., Milana, M., O'Brien, A., Rebre, S., Rijk, R., and Piringer, O., Evaluation of migration models that might be used in support of regulations for food-contact plastics. *Food Addit. Contam.,* (2005) 22: 73–90.

11. Qin, Y., Rubino, M., Auras, R., and Lim, L.-T., Impact of polymer processing on sorption of benzaldehyde vapor in amorphous and semicrystalline polypropylene. *J. Appl. Polym. Sci.,* (2008) 110: 1509–1514.

12. Jonquieres, A. and Fane, A., Modified BET models for modeling water vapor sorption in hydrophilic glassy polymers and systems deviating strongly from ideality. *J. Appl. Polym. Sci.,* (1998) 67: 1415–1430.

13. Feng, H., Modeling of vapor sorption in glassy polymers using a new dual mode sorption model based on multilayer sorption theory. *Polymer,* (2007) 48: 2988–3002.

14. Favre, E., Nguyen, Q. T., Clément, R., and Néel, J., The engaged species induced clustering (ENSIC) model: a unified mechanistic approach of sorption phenomena in polymers. *J. Membrane Sci.,* (1996) 117: 227–236.

15. Dhoot, S. N., *Sorption and transport of gases and organic vapors in poly(ethylene terephthalate)*. 2004, The University of Texas at Austin.

16. Dury-Brun, C., Hirata, Y., Guillard, V., Ducruet, V., Chalier, P., and Voilley, A., Ethyl hexanoate transfer in paper and plastic food packaging by sorption and permeation experiments. *J. Food Eng.,* (2008) 89: 217–226.

17. Cooksey, K., Important factors for selecting food packaging materials based on permeability. *Flexible Packaging Conference*, *2004*.

Chapter 6

Conclusions and recommendations

6.1 Conclusions

Mineral oil (MO) present in paper packaging and its subsequent migration into foodstuff, even in the presence of a plastic protective liner between the board and the food, was recently reported. The presence of MO in foodstuff is alarming, as it consists of a complex mixture of compounds, including low quantities of aromatic MO, of which the toxicological effects are largely unknown. This type of contamination was not perceived as a food safety issue in the past, as it was not measurable due to limitations of analytical techniques. The reason for this is the extremely low concentrations of the MO contaminants in the packaging material, as well as the difficulty in separating them from other hydrocarbons. In addition, migration testing into food is a lengthy procedure which has not been well reported on for MO thus far. Therefore, there exists a need for a simple test method which not only allows the packaging industry to evaluate their products for food safety, but also a method that could assist in the product development of suitable MO barriers.

This work reports on a new test method to predict the migration of volatile organic contaminants from packaging materials into foodstuffs. This method has been designed to afford measurable permeation rates within a short period of time. The transport of contaminants through the barrier materials considered has been accelerated using a dual strategy, namely:

1. by using a MO simulant with a high capability to diffuse through polymeric materials, and
2. by using a high concentration gradient in the permeation cell from saturated vapours to a zero vapour pressure inside the cell. This was achieved by immersing into a saturated chamber (with the penetrant vapour) a permeation cell containing a fast organic vapours adsorbent material.

The method was validated using activated carbon as adsorbent material, and heptane vapour as a MO simulant. By measuring the flow of organic vapour, referred to as the heptane vapour transmission rate, through model packaging materials, a wide variety of polymer films and paper coatings, commonly used as materials in food contact applications, was characterised in terms of their barrier properties towards MO migration. This was based on the correlation found between the results from HVTR and MOVTR, the latter referring to actual MO being used to generate a saturated

environment in the permeation method, in stead of the MO simulant, heptane. Furthermore, the diffusion coefficient of MO in model packaging materials could be derived from data obtained by the new permeation method which, in turn, was utilised to estimate the MO migration behaviour in real conditions of use of the packaging materials, and subsequent prediction of product shelf-life.

A more comprehensive study of the transport parameters of the model packaging materials was performed by gravimetric heptane vapour sorption experiments. An evaluation of the diffusion coefficients, solubility coefficients, and permeability coefficients, over a wide range of penetrant partial pressures, revealed that overall permeability of the materials was mostly controlled by diffusion, even though for some materials the effect of solubility was more evident at high partial pressures. Sorption kinetics gave more information regarding rate of vapour sorption, and the extent of equilibrium mass uptake, whereas sorption fitting to a dual mode sorption model gave details on polymer-penetrant interactions. This data is useful in the case of MO barrier product development, but not a necessity to evaluate the MO barrier materials, which can be done independently with the HVTR permeation method.

Classification of barrier materials in terms of its efficiency to protect foodstuff against MO migration according to HVTR was found to be in the order PET > PP > coated PB > polyethylenes, > and uncoated PB. A mathematical model based on diffusion, recognised by EU regulation to predict migration of contaminants from packaging into foodstuff, was used to predict product shelf-life to clarify even further the HVTR classification of barrier materials. The significance of this model was verified by the findings from vapour sorption that showed that permeability of the materials was mostly controlled by diffusion. In addition, higher permeability coefficients obtained with the permeation method, as compared to permeability coefficients obtained from vapour sorption experiments over the entire pressure range, demonstrated that the permeation method gives “worst case scenario” values used to derive transport parameters for actual MO migration.

One of the major advantages of the new permeation test method is that it is a simple method that can be carried out in a few hours, as opposed to actual MO migration testing of barrier materials which could take several months for completion, and requires costly and highly specialised analytical equipment. The HVTR method has proved to give meaningful results within as little as 1 h testing time, although there is a limitation for very good MO barrier materials for which the exposure time should be

increased to a few hours. Packaging manufacturers may hence afford using the present method disclosed in this work as a quality control tool to monitor the MO barrier properties of their products on a regular basis. Furthermore, a “worst case” shelf-life can be predicted from which a safe margin for use of the packaging material can be derived from. This adds value to the fact that the method can be used in the development of barrier materials for MO migration, as migration studies and shelf-life predictions during the product development process can now be performed much faster.

An additional advantage of this method is that the simulant used (i.e. heptane) can also be correlated to other organic compounds present in packaging materials, for which the migration needs to be controlled. Alternatively, the penetrant simulant used in this study may also be replaced by any other volatile organic compound of interest, allowing performing accurate migration studies way beyond mineral oils.

6.2 Recommendations for future work

The best way to validate the new HVTR method would be to compare the results obtained, to actual MO migration from these packaging materials. This could be done by spiking the packaging samples with MO, and monitoring the MO concentration in a food simulant as a function of time. However, this will require more sensitive analytical methods, since more realistic concentrations of MO resembling actual concentrations found in packaging materials are too low to evaluate gravimetrically, and require the use of advanced chromatographic equipment.

This study was based on dry food packaging materials at room temperature, since these are the types of products mostly affected by the concerns of MO migration. However, it would be of great value to extend the work to investigations at different temperatures, as these foods can be exposed to higher or lower temperatures during transport and storage.

As mentioned in the conclusions, this test method is not restricted to simply heptane and mineral oil vapour. It is versatile in the sense that any volatile organic compound could be utilised in order to determine its transmission rate through packaging materials. The proposed permeation method would gain even more significance if HVTR could be correlated to transmission rates of other migrating species considered a food contaminant present in packaging materials.